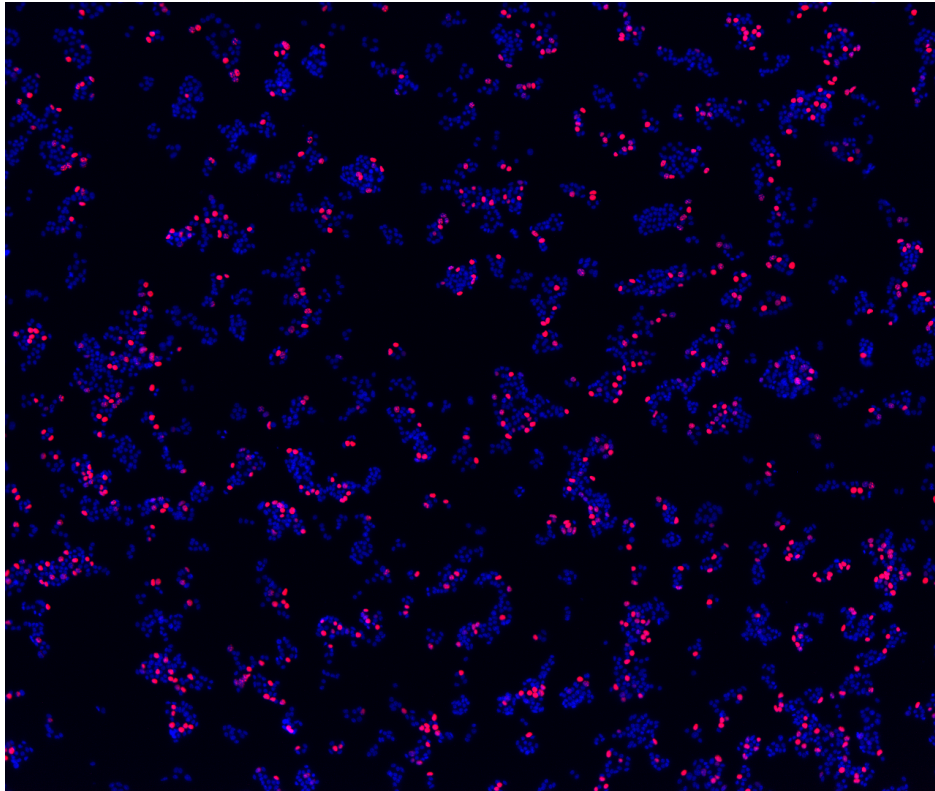




**CHALMERS**  
UNIVERSITY OF TECHNOLOGY

---



# **Validation of a novel drug target in type 2 diabetes mellitus**

Master's thesis in Biotechnology

**IDA ALEXANDERSSON**



MASTER'S THESIS 2017

**Validation of a novel drug target  
in type 2 diabetes mellitus**

IDA ALEXANDERSSON



**CHALMERS**  
UNIVERSITY OF TECHNOLOGY

Department of Biology and Biological Engineering  
*Division of Systems and Synthetic Biology*  
CHALMERS UNIVERSITY OF TECHNOLOGY  
Gothenburg, Sweden 2017

Validation of a novel drug target  
in type 2 diabetes mellitus  
Ida Alexandersson

© IDA ALEXANDERSSON, 2017.

Supervisor: Björn Tyrberg, Department of Translational Science, AstraZeneca  
Examiner: Christer Larsson, Department of Biology and Biological Engineering,  
Chalmers University of Technology

Master's Thesis 2017  
Department of Biology and Biological Engineering  
Division of Systems and Synthetic Biology  
Chalmers University of Technology  
SE-412 96 Gothenburg  
Telephone +46 31 772 1000

Cover: Measurement of proliferation in MIN6 cells. Synthesized DNA labeled with EdU bound to fluorophore Alexa Fluor®647 (red) and nuclei stained with HCS NuclearMask<sup>TM</sup> Blue stain (blue).

Typeset in L<sup>A</sup>T<sub>E</sub>X  
Gothenburg, Sweden 2017

## Abstract

Type 2 diabetes (T2DM) is characterized by altered insulin secretion as a result of progressive functional failure of pancreatic  $\beta$ -cells. Genetics is known to be a factor in the pathophysiology of the disease, and several genomic loci have been identified with T2DM susceptibility. Polymorphisms in the gene encoding Target X is associated with T2DM and the expression of the gene is further upregulated in pancreatic T2DM  $\beta$ -cells. In this study, the mechanism linking an increased expression of Target X to T2DM was evaluated. Overexpression of Target X was achieved with adenoviral transduction. The gene was overexpressed in two  $\beta$ -cell lines, EndoC- $\beta$ H1 and MIN6. Functional assays evaluating glucose stimulated insulin secretion (GSIS), proliferation and apoptosis in response to overexpressing Target X were performed with both cell lines. Upregulated gene expression of Target X in EndoC- $\beta$ H1 cells resulted in a reduction in cytokine induced apoptosis compared to control. Moreover, it returned an increased fold-response in GSIS. Even though a trend of increased apoptosis was observed with the MIN6 cells, there was no significant difference compared to control samples. Contrary to the results with EndoC- $\beta$ H1 cells, a significant decrease in fold-response in the GSIS assay was observed with MIN6 cells. No impact of overexpression of Target X on proliferation was observed with any of the two cell lines. Nevertheless, qPCR analyses revealed a low fold increase in mRNA expression in MIN6 cells compared to EndoC- $\beta$ H1 cells. In conclusion, this study gave further insight into the linkage between upregulation of Target X and T2DM by suggesting that it may influence  $\beta$ -cell survival and insulin secretion.

Keywords: Type 2 diabetes, target validation,  $\beta$ -cell, EndoC- $\beta$ H1, MIN6, polymorphisms, GSIS, apoptosis, proliferation.



## Acknowledgements

I would first like to thank my supervisor Björn Tyrberg for allowing me to be part of his project and for all the support and guidance during my time at AstraZeneca. Further, I would like to thank Alex Zhou for your support, patience and help throughout this master's thesis project and for always taking your time to answer my endless questions. I would also like to thank all the staff in the cell biology team at the department of Translational Science at AstraZeneca as well as the other diploma workers. Thank you for being so welcome to me and for all your support. Last, but not least, I would like to thank my dear family and friends for always believing in me and for your encouragement during this master's thesis project and throughout my years of studying.

Thank you.

Ida Alexandersson, Gothenburg, June 2017



## Abbreviations

<b>1-AKP</b>	1-Azakenpaullone
<b>ADP</b>	Adenosine diphosphate
<b>ATP</b>	Adenosine triphosphate
<b>BSA</b>	Bovine serum albumin
<b>CMV</b>	Cytomegalovirus
<b>CT</b>	Threshold Cycle
<b>DAG</b>	Diacylglycerol
<b>DMSO</b>	Dimethyl sulfoxide
<b>eQTL</b>	Expression quantitative trait loci
<b>ER</b>	Endoplasmic Reticulum
<b>FAM</b>	6-Carboxyfluorescein
<b>FBS</b>	Fetal bovine serum
<b>FRET</b>	Fluorescence Energy Transfer
<b>GAPDH</b>	Glyceraldehyde-3-phosphate Dehydrogenase
<b>GLUT</b>	Glucose transporter
<b>GSIS</b>	Glucose stimulated insulin secretion
<b>GSK3</b>	Glycogen Synthase Kinase-3
<b>GWAS</b>	Genome-wide association study
<b>HTRF</b>	Homogenous Time-Resolved Fluorescence
<b>IBMX</b>	3-isobutyl-1-methylxanthine
<b>MGB</b>	Minor groove binder
<b>MOI</b>	Multiplicity of infection
<b>qPCR</b>	Quantitative Real-time Polymerase Chain Reaction
<b>SGLT2</b>	Sodium-glucose co-transporter 2
<b>SNP</b>	Single nucleotide polymorphism
<b>TCA</b>	Tricarboxylic Cycle
<b>T1DM</b>	Type 1 Diabetes Mellitus
<b>T2DM</b>	Type 2 Diabetes Mellitus
<b>TS</b>	Translational Science



# Contents

<b>1</b>	<b>Introduction</b>	<b>1</b>
1.1	Confidentiality . . . . .	2
1.2	Aim . . . . .	2
<b>2</b>	<b>Background</b>	<b>3</b>
<b>3</b>	<b>Theory</b>	<b>5</b>
3.1	The Pancreas . . . . .	5
3.2	Glucose Homeostasis . . . . .	6
3.3	Glucose Stimulated Insulin Secretion (GSIS) from $\beta$ -cells . . . . .	7
3.4	Type 2 Diabetes Mellitus (T2DM) . . . . .	7
3.5	$\beta$ -cells in Human Type 2 Diabetes . . . . .	8
3.6	Genetic theoretical concepts . . . . .	9
3.6.1	Single nucleotide polymorphism (SNP) . . . . .	9
3.6.2	Genome-Wide Association Studies (GWAs) . . . . .	10
3.6.3	Expression quantitative trait loci (eQTL) . . . . .	10
3.7	Cell lines . . . . .	11
3.7.1	EndoC- $\beta$ H1 cells . . . . .	11
3.7.2	MIN6 cells . . . . .	11
3.8	Techniques & Functional assays . . . . .	11
3.8.1	Adenoviral transduction . . . . .	11
3.8.2	Quantitative real-time PCR . . . . .	12
3.8.3	Homogeneous Time-Resolved Fluorescence . . . . .	13
3.8.4	Apoptosis Assay . . . . .	13
3.8.5	Proliferation assay . . . . .	14
<b>4</b>	<b>Materials &amp; Methods</b>	<b>15</b>
4.1	Cell culture: EndoC- $\beta$ H1 . . . . .	15
4.2	Cell culture: MIN6 . . . . .	15
4.3	Adenoviral vectors . . . . .	15
4.4	Selection of adenoviral concentration for overexpression . . . . .	16
4.4.1	RNA extraction . . . . .	16
4.4.2	Quantitative PCR (qPCR) . . . . .	16
4.5	Apoptosis Assay . . . . .	17
4.6	Glucose Stimulated Insulin Secretion Assay . . . . .	17
4.7	Proliferation assay . . . . .	18

4.7.1	EndoC- $\beta$ H1 cells . . . . .	18
4.7.2	MIN6 cells . . . . .	19
<b>5</b>	<b>Results &amp; Discussion</b>	<b>21</b>
5.1	Determination of adenoviral concentrations for overexpression of Target X . . . . .	21
5.2	Apoptosis assay . . . . .	23
5.3	Proliferation assay . . . . .	26
5.4	Glucose stimulated insulin secretion assay . . . . .	28
5.5	Comparison of results with EndoC- $\beta$ H1 & MIN6 . . . . .	31
<b>6</b>	<b>Conclusions &amp; Outlook</b>	<b>33</b>
6.1	Conclusions . . . . .	33
6.2	Outlook . . . . .	33
	<b>Bibliography</b>	<b>35</b>
<b>A</b>	<b>Appendix</b>	<b>I</b>
<b>B</b>	<b>Appendix</b>	<b>III</b>
<b>C</b>	<b>Appendix</b>	<b>V</b>
<b>D</b>	<b>Appendix</b>	<b>VII</b>

# 1

## Introduction

The human pancreas is a gland with both exocrine and endocrine functions. Within the pancreas, clusters of endocrine cells form micro-organs called islets of Langerhans. These micro-organs are important in regulation of glucose homeostasis through insulin and glucagon secretion [1]. They consists of at least five different cell types of which  $\beta$ -cells constitutes to the majority of the cell mass. The primary role of  $\beta$ -cells is to secrete insulin, a peptide which is important in regulation of blood glucose and nutrient uptake [1].  $\beta$ -cell failure and dysfunction can trigger the development of diabetes mellitus; a chronic, metabolic disease characterized by abnormally high blood glucose levels, hyperglycemia, and disturbances in metabolism of fat, carbohydrates and proteins. Diabetes mellitus is classified into different types of which type 2 is the most common. Type 2 diabetes (T2DM) is characterized by dysfunctions of both insulin secretion by the pancreatic  $\beta$ -cells and a often coexisting development of resistance to insulin action in insulin-dependent tissues [2]. The consequences of the disease can be disabling complications including blindness, organ failure and, in the absence of treatment, death [3].

Lifestyle, environmental factors and genetics are interacting causes in the development of T2DM [4]. Genome-wide association studies (GWAS) have enabled the detection of several associations between development of T2DM and specific genomic loci. A majority of the genes that have been found to associate with development of T2DM have also been found to be expressed in pancreatic  $\beta$ -cells [1]. The pharmacological treatments of diabetes available on the market today are based on symptomatic relief rather than modification of the disease itself. This results in an unmet need for the development of new drugs that are modifying the disease to prevent long-term disabling complication and increase patient quality of life. By studying and validating the genetic polymorphisms associated with T2DM, novel drug targets that rescue and regenerate failing  $\beta$ -cells, as well as combat insulin resistance, could potentially be discovered.

From GWAS, two genetic variants (*i.e.* single nucleotide polymorphisms (SNPs)) of a gene encoding Target X have been associated with development of T2DM. Further, the SNPs have been found to be linked to increased expression of Target X in pancreatic  $\beta$ -cells from T2DM donors. The goal of this master thesis project was to experimentally validate Target X as a potential drug target in T2DM and to further increase the understanding of the biological role and function of Target X in pancreatic  $\beta$ -cells. The functional role of the target was studied in response to overexpression of the gene encoding Target X, which was accomplished by adenovi-

ral transduction. Validation of how an upregulation of Target X impacts pancreatic  $\beta$ -cell function was evaluated in three functional assays studying apoptosis, glucose stimulated insulin secretion and proliferation. The studies have been conducted in both a human  $\beta$ -cell line, EndoC- $\beta$ H1, and a mouse  $\beta$ -cell line, MIN6. Experiments and techniques used includes mammalian cell culturing, qPCR analysis, HTRF immunoassay and adenoviral transduction. Taken together, this project have aided to increase the understanding of the potential functional role of Target X in pancreatic  $\beta$ -cells.

### 1.1 Confidentiality

This study is part of ongoing research at AstraZeneca. Hence, some of the facts and information regarding Target X will not be stated in this report due to confidentiality. The real gene name of the target will not be revealed, and the target will be referred to as Target X. Further, articles in which the gene name is mentioned will not be referred to.

### 1.2 Aim

The aim of this study was to experimentally validate Target X *in vitro* as a potential drug target in T2DM. Further, this project aimed to increase the understanding of the connecting mechanism between an upregulation in gene expression of Target X and T2DM, as well as of the function of Target X in pancreatic  $\beta$ -cells.

# 2

## Background

AstraZeneca is a global biopharmaceutical company engaged in the discovery, development, manufacturing and marketing of prescription medicines. Within CVMD (Cardiovascular and Metabolic Diseases) at AstraZeneca, the Translational Science (TS) department drives novel target validation from human genetics. The unmet need for novel drugs with a disease mechanism target in diabetes is the reason behind the focus of the Cell biology team within TS to deliver novel target proposals with strong genetic and experimental validation. The bioinformatics team within TS has, together with the Cell biology team, generated hypotheses based on human genetics and omics data for novel targets with disease modifying effects in diabetes.

From GWAS, two genetic variants of a gene encoding Target X has been associated with development of T2DM. Both variants are SNPs in non-coding regions of the gene. Further, a study of gene expression in human islets using expression quantitative trait locus (eQTL) data, among other genes the two genetic variants were found to be linked to increased expression of Target X in human islets. In analyses at AstraZeneca of RNA sequencing data from single-cell transcriptome profiling of human pancreatic islets, it was revealed that mRNA expression of Target X is enriched in  $\beta$ -cells in comparison to the other endocrine cell types in islets of Langerhans, see figure 2.2 (a). Further, it was found that mRNA expression of Target X is significantly upregulated in pancreatic  $\beta$ -cells from donors with T2DM compared to healthy  $\beta$ -cells. The linkages between SNPs, GWAS and eQTLs are visualized in figure 2.1, and the concepts are further explained in sections 3.6.1, 3.6.2 and 3.6.3. That there is a correlation between an upregulation in gene expression (eQTL) of Target X and T2DM is consequently known, but the mechanism behind the connection remains to be elucidated. In this master thesis project, the function of Target X was evaluated when overexpressing the gene to simulate the disease state.

## 2. Background

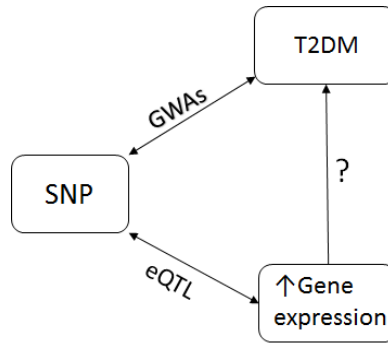


**Figure 2.1:** Displays the linkage between single nucleotide polymorphisms (SNPs), type 2 diabetes and an upregulation in gene expression via GWAS and eQTLs.

The Target X gene encodes a protein involved in lipid metabolism downstream of diacylglycerol (DAG). Other details about the biological function of Target X that is known today will not be stated in this report due to confidentiality. Further, two splice variants of Target X have been found that differ in length with one exon. The mRNA expression levels of the two splice variants of Target X in EndoC- $\beta$ H1 cells and in human islets have been measured prior to this master's thesis project at AstraZeneca. As seen in figure 2.2 (b), the most abundantly expressed splice variant in healthy human islets is splice variant 1. Hence, that is the splice variant that was overexpressed in this study. A vector containing green fluorescent protein (GFP) was used as control.

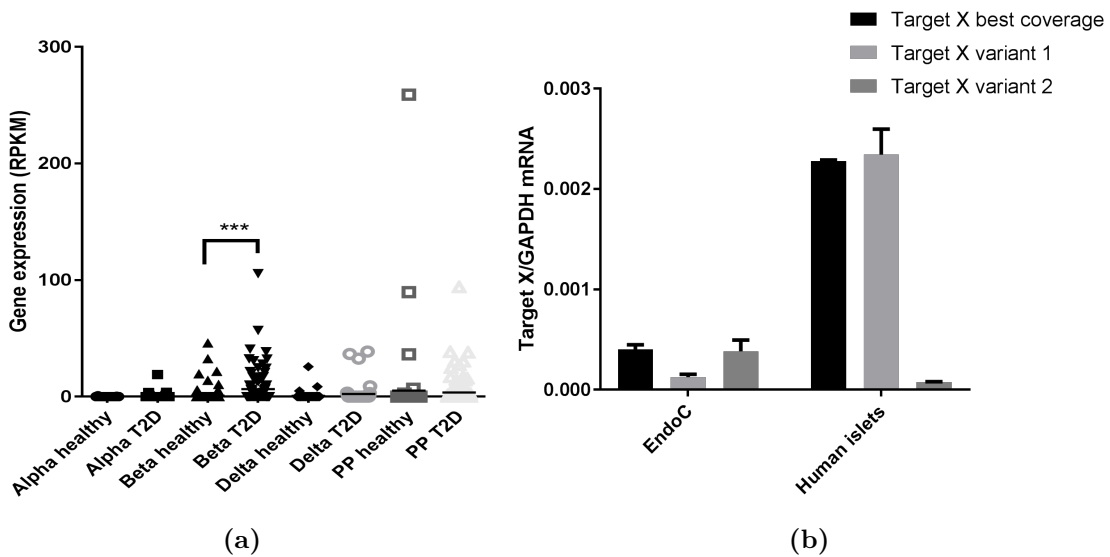


**Figure 2.2:** Displays preliminary data. In (a), mRNA expression of Target X measured with RNAseq in all endocrine cell types in Islets of Langerhans from healthy and T2D patients. In (b), mRNA expression of the two splice variants of Target X in EndoC- $\beta$ H1 cells and human islets. Best coverage indicates that the probe used detects both splice variants. Error bars represent standard deviation. \*\*\* denotes a significant level of  $p \leq 0.001$ . Image courtesy of Björn Tyrberg and Alex Zhou, Translational Science, AstraZeneca.

# 3

## Theory

This section describes the function and role of the pancreas and more specifically the endocrine cell types in islets of Langerhans. The regulation of glucose homeostasis and glucose stimulated insulin secretion are outlined. Further, this section describes the characteristics and the pathogenesis of T2DM and the role and dysfunctions of pancreatic  $\beta$ -cells in the development of the disease. Theory describing the main concepts to the genetic background of Target X; genome wide association studies, single nucleotide polymorphisms and expression quantitative trait loci are outlined. Furthermore, the two cell lines, and background to the techniques and functional assays used in the study are described in this section.

### 3.1 The Pancreas

The human pancreas is a gland with both exocrine and endocrine features and with two main functions: glucose homeostasis and digestion of proteins, lipids and fats [5]. It is located in the retroperitoneal space in the abdominal cavity. Pancreas is commonly divided into three parts head, body and tail [5]. It is composed of small lobules, which in turn consists of ductules and clusters of cells. The major part of the pancreas (98% of the parenchyma) is devoted to its exocrine function [1]. The exocrine cells in the pancreas form cell clusters called acini, and produce digestive enzymes and bicarbonate that are secreted by exocytosis to the acinar lumen. From the acinar lumen the products are transported into the pancreatic duct (or Wirsburg duct), which combine with the common bile duct, into the duodenum [1]. To avoid damage of the cell and digestion of the pancreas by the digestive enzymes, they are synthesized and stored in inactive forms and packed in granules inhibiting their activity. The inactive proenzymes are converted to their active forms by other enzymes when entering the duodenum. The main enzymes secreted are amylase, lipases and proteases [6].

Clusters of endocrine cells form micro-organs called islets of Langerhans (named after Paul Langerhans that discovered them in 1869) that constitutes 1-2% of the pancreatic parenchyma [5]. The main function of the islets of Langerhans is as a key regulator of glucose homeostasis by production of insulin. Approximately one million islets are scattered throughout the exocrine tissue [5]. The islets vary in size from larger aggregates to only a few cells with a mean diameter of 140 $\mu$ m. Islets are encapsulated in a thin layer of connective tissue and are infiltrated by a compact network of capillaries facilitating the endocrine cells to sense and respond to

nutrient-levels in the circulating blood [1]. The human islets consists of at least five different endocrine cell types [1]. The predominant endocrine cell type is the  $\beta$ -cell consisting for 50-60% of the islet mass.  $\beta$ -cells produces insulin and islet amyloid polypeptide. The second most abundant endocrine cell type is the glucagon secreting  $\alpha$ -cell. Glucagon is important in regulation of hypoglycemia by stimulating hepatic glucose production, acting in an opposite manner to insulin [7].  $\delta$ -cells, the third endocrine cell type, secretes somatostatin. Somatostatin represses both insulin and glucagon secretion by acting on receptors on  $\alpha$ - and  $\beta$ -cells [7].  $\gamma$ -cells, or pancreatic polypeptide-producing F-cells, produce pancreatic polypeptide. Although studies have suggested involvement of pancreatic polypeptide regulation of food intake and energy metabolism, the function still remains less established [8]. The least abundant endocrine cell type in the islets are  $\epsilon$ -cells producing the hormone ghrelin [7].

## 3.2 Glucose Homeostasis

Glucose is the preferred source for energy of most tissues and organs in the human body. It is formed when poly- and oligosaccharides from food intake are digested and is further also generated by liver and kidney in gluconeogenesis [9]. Long-term elevated blood glucose concentrations can cause complications such as renal failure, blindness or neuropathy. Further, too low blood glucose levels can cause loss of consciousness, seizures or even death [9]. Subsequently, blood glucose concentrations in the body needs to be tightly regulated by several factors to be kept within a narrow range (around 5 mM). The term glucose homeostasis is used to describe the regulatory mechanism of keeping blood glucose levels in the body within this range. Insulin and glucagon, secreted by pancreatic endocrine cells, are two important key regulators of glucose homeostasis working in opposed manner to each other [9].

Immediately after intake of a meal, blood glucose levels begin to rise. As a response to increased concentrations of blood glucose, pancreatic  $\beta$ -cells increase the secretion of insulin. By binding of insulin to membrane-receptors of cells, primarily in adipose, liver and muscle tissue, the uptake of glucose by cells is distinctly increased [10]. Insulin stimulates activated muscles to increase their uptake of glucose and use it as energy. If the muscles are at rest, the glucose is stored as glycogen and can later be used as a source of energy. Insulin also stimulates hepatic uptake and storage of glucose by several actions e.g. by promoting hepatic glycogen synthesis [10]. In an opposed manner to insulin secretion by  $\beta$ -cells, the hyperglycemic hormone glucagon is secreted by  $\alpha$ -cells as a response to low blood glucose levels [11]. Insulin and glucagon acts as important feedback systems to each other to keep blood glucose within normal levels. Glucagon increases gluconeogenesis in the liver by activating enzymes important in the synthesis and in transport and uptake of amino acids. Further, glucagon stimulates glycogenolysis (*i.e.* breakdown of glycogen) in the liver. Both actions results in released glucose into the blood stream [10].

### 3.3 Glucose Stimulated Insulin Secretion (GSIS) from $\beta$ -cells

Pancreatic  $\beta$ -cells sense elevated extracellular glucose levels and transports it across plasma membrane through facilitative glucose transporters GLUT (GLUT-1 in humans) [1]. Glucose is subsequently phosphorylated by glucokinase, and converted into pyruvate by the glycolytic pathway. Subsequently, pyruvate is converted to acetyl-CoA, which enters the tricarboxylic cycle (TCA) in mitochondria [12]. Transportation of glucose into pancreatic  $\beta$ -cells, increases the glycolytic flux and TCA cycle activity resulting in increased ATP production in mitochondria [1]. Production of ATP increases the cellular ATP to ADP ratio causing the ATP-sensitive potassium channels ( $K^+_{ATP}$  channels) in the plasma membrane to close [13]. At low extracellular glucose levels, the  $K^+_{ATP}$  channels are open allowing an efflux of  $K^+$  ions along their concentration gradient. The efflux maintains a hyperpolarized membrane potential of the  $\beta$ -cells. An elevation in glucose levels and increased ATP to ADP ratio, causes closure of the  $K^+_{ATP}$  channels and depolarization of the membrane [1, 13]. A subsequent effect of the depolarization is opening of voltage-gated  $Ca^{2+}$  channels resulting in an influx of  $Ca^{2+}$  ions into the cells. The intracellular increase in  $Ca^{2+}$  levels consequently triggers exocytosis of insulin-containing granules [1, 14].

### 3.4 Type 2 Diabetes Mellitus (T2DM)

Diabetes mellitus is a metabolic disorder characterized by hyperglycemia (*i.e.* abnormally high blood glucose), and disturbances in metabolism of fat, carbohydrate and protein resulting from impaired secretion of insulin, insulin action, or both [2]. Characteristic symptoms of diabetes such as thirst, blurred vision and weight loss may be present if not treated. Further, increased susceptibility to infections and impaired growth can be indications of diabetes. Symptoms of the disease may be absent, or can in more severe forms of the disease result in ketoacidosis, coma or in absence of treatment, death [15]. Diabetes mellitus is classified into different types of which type 1 and type 2 are the more common. Type 1 diabetes (T1DM) is characterized by the destruction of pancreatic  $\beta$ -cells by autoimmune processes resulting in an absolute deficiency of insulin [2]. Type 2 diabetes (T2DM), the most common type of diabetes mellitus (about 90% of all cases), is characterized by dysfunctions of both insulin secretion and development of resistance to insulin action in peripheral tissues [2]. T2DM is a complex disease and the complete pathophysiology remains to be fully elucidated. The role of insulin resistance and altered insulin secretion due to dysfunctional  $\beta$ -cells in development of T2DM has been debated [16]. Insulin secreted from  $\beta$ -cells is regulated by glucose concentrations in the blood, and signals to insulin-sensitive tissues to increase glucose uptake and suppress glucose production. Hence, when insulin resistance develop,  $\beta$ -cells increase their insulin secretion to maintain normal glucose concentrations. When  $\beta$ -cell function declines, they are no longer capable of maintaining glucose homeostasis and glucose levels raise, leading to hyperglycemia [16].

Incidence of T2DM is affected by lifestyle, environmental factors and genetics [4]. Main lifestyle factors associated with increased risk of disease are a high-energy diet, obesity and a sedentary lifestyle [17]. It has been observed that in persons at high risk of development of T2DM, changes in lifestyle with increased physical activity, healthier diet and weight loss can prevent or delay development of the disease [18]. Further, T2DM is highly inheritable. From genetic studies, such as GWAS, several genomic loci have been identified to be associated with development of T2DM contributing to increased understanding of how genes are influencing the pathophysiology of the disease [19].

T2DM and severe hyperglycemia often develops gradually and it may remain undiagnosed for years. Initially, most patients with T2DM do not need insulin treatment and a healthy diet and physical activity may slow down the progression of the disease [2]. In more severe cases and when  $\beta$ -cell failure has progressed further, drugs that lower and maintain glucose concentrations might be necessary to manage the disease. The prevalence of T2DM has increased the research and development of new therapies and there are drugs available today with different targets and actions to treat hyperglycemia [16]. For example, a commonly prescribed drug in treatment of T2DM is Metformin that belongs to a class of anti-diabetic drugs called Biguanides. The main effect of Metformin is to decrease hepatic gluconeogenesis and increase insulin sensitivity, thus, helps control blood glucose levels [20]. Another example of drugs are inhibitors of sodium-glucose co-transporter 2 (SGLT2) that decreases the amount of glucose reabsorbed from urine [16].

### 3.5 $\beta$ -cells in Human Type 2 Diabetes

That a reduction in total  $\beta$ -cell mass is central in development of T2DM is supported by several studies [3, 21]. A study by Sakaruba *et al.* [22], reported a reduction in  $\beta$ -cell density and a 30% reduction in  $\beta$ -cell mass when comparing human islets samples from diabetic and non-diabetic patients. The reasons for development of  $\beta$ -cell deficit in T2DM is less well established. However, increased frequency of  $\beta$ -cell apoptosis is generally assumed to be a main contributor to decreased  $\beta$ -cell mass [3]. Several factors have been related to induction of apoptosis in  $\beta$ -cells. High glucose concentration and elevated free fatty acid levels, two features commonly associated with characteristics of T2DM, have been linked to reduced proliferative capacity and increased apoptosis of  $\beta$ -cells in human islets [23]. Further, endoplasmic reticulum (ER) stress leading to accumulation of unfolded or misfolded proteins activates apoptotic pathways contributing to increased  $\beta$ -cell deficit [24]. In addition, increased levels of reactive oxygen and nitrogen species inducing oxidative stress has in both animal and human T2DM-models been linked to increased apoptosis and reduced secretory capability of  $\beta$ -cells [25]. Antioxidant defense capacity in  $\beta$ -cells are low, consequently, these cells are susceptible to elevated oxidative stress [25]. Elevated levels of  $\beta$ -cell death morphologically distinct from apoptosis has also been found to associate with altered autophagy, a regulated process of removing and re-

cycling dysfunctional components in the cell [26]. Marked autophagy may induce non-apoptotic cell death. These results implies that other cell death pathways than apoptosis may be contributing to elevated  $\beta$ -cell death in T2DM [26]. Moreover, the decrease in  $\beta$ -cell mass as a result of increased apoptosis does not seem to be compensated for by increased regenerative capacity in the islets. It has been reported that the rate of both  $\beta$ -cell replication and islet neogenesis (*i.e* formation of new islets) measured in pancreatic autopsy samples remain similar between T2DM samples and controls [3].

Several functional defects of pancreatic T2DM  $\beta$ -cells have also been discovered. Insulin secretion in response to elevated glucose concentrations (16.7 mM) has been reported to be markedly lower in T2DM islets compared to controls [27]. Further, it was in the same study also shown that expression levels of glucose transporters, GLUT-1 and GLUT-2, responsible of transporting glucose over the plasma membrane are reduced in T2DM islets. In addition to altered insulin secretion, mitochondrial defects have also been reported. As has been described, intracellular ATP/ADP ratio in pancreatic  $\beta$ -cells plays a crucial role in GSIS. In a study by M. Anello *et al.* [28], islets from diabetic donors were not capable of increasing their adenine nucleotide (ATP) content in response to elevated glucose levels (16.7 mM). As a consequence, the ATP/ADP ratio were lower in these islets compared to controls which could contribute to the altered secretory response to glucose observed.

## 3.6 Genetic theoretical concepts

### 3.6.1 Single nucleotide polymorphism (SNP)

The most common form of genetic variants in the human genome are single nucleotide polymorphisms (SNPs) [29]. A SNP is a single base-pair change in the DNA sequence of a gene that occur with high frequency in a population (in more than 1%) [30]. The different forms of a SNP are called alleles. SNPs can lead to phenotypic changes by occurring in coding sequences of a gene and thus cause changes in the amino acid sequence of a protein. However, SNPs also occurs in non-coding sequences of genes, which is a less well-studied type of genetic variants. The non-coding sequences of a gene, such as the 3' untranslated region (3'UTR) of mRNAs, often contains functional sequence elements that are important in transcription of a gene and gene regulation [30]. SNPs in such regions can cause changes to the stability of mRNA transcript or affect gene expression by up- or down-regulating a gene. Example of elements in non-coding regions that can be affected are microRNA target sites [30]. MicroRNAs are important elements in gene silencing by binding to a target mRNA, bringing RNA-induced silencing complex (RISC) and allowing the gene expression to be repressed. Further, the 3'UTR region contains sequence elements regulating polyadenylation of mRNA [29, 30]. The two genetic variants of Target X are SNPs in non-coding regions linked to increased expression of the gene.

### 3.6.2 Genome-Wide Association Studies (GWAs)

Genome-wide Association Studies (GWAs) have become a powerful tool for investigation of how genetics are associated with complex diseases [29]. In GWAs, large sets of SNPs are assayed for association with a trait or a disease. A GWA study is typically carried out with two groups of people, one group with the disease being studied, and one group of healthy people [31]. The genomes of all participants are sequenced and scanned for specific genetic markers and genetic variants. For all genetic variants, the allele frequency is examined between the two groups. If a genetic variant is significantly more common in individuals with the disease compared to individuals in the other group, the genetic variant is said to be associated with the disease. GWA studies have revolutionized the identification of genetic risk factors in common and complex diseases and have contributed to the field of personalized medicine in pharmacology [29, 31].

### 3.6.3 Expression quantitative trait loci (eQTL)

Genetic studies have enabled detection of genetic variants that regulates gene expression. Expression quantitative trait loci (eQTL) are variants (SNPs) of DNA sequences in the genome that affects the expression level of one or more genes [32]. The term QTLs refers to loci in the genome that correlates with a specific trait (e.g. risk of disease). With eQTLs, the trait that is being studied is gene expression. By studying the genetic differences between individuals in populations, eQTLs can be identified. The genome of each individual needs to be sequenced followed by a measurement of the expression of each gene in each individual by either RNA sequencing or expression microarray. After analysis of sequencing data, individuals are subsequently grouped according to the allele of the SNP they carry. Using statistical tests, significant variations in gene expression between groups and alleles can be identified. Logarithm of odds (LOD) is a score that indicates if a statistical linkage exists between mRNA level and genotype. If the LOD score of a region is high, that indicates that there is a significant variation in mRNA levels between the inherited alleles between groups, then that region is called an eQTL [32]. eQTLs can be divided into local or distant eQTLs. If the eQTL influence gene expression of genes nearby, the eQTL is local. Further, local eQTLs can influence gene expression either as a cis-eQTL or a trans-eQTL. A cis-eQTL affects the expression of only the copy of a gene that is located on the same chromosome as the eQTL. That is, the copy of the gene at one of the two copies of a chromosome inherited from both parents. A trans-eQTL on the other hand, influence the function, expression or structure of a factor that in turn alter the expression of a gene. If a trans-eQTL regulates a gene near to it, it is a local trans-eQTL. If an eQTL instead regulates a gene that is not located near it but further away, it is defined as a distant eQTL. The majority of distant eQTLs are trans-eQTLs. So far, the most common type of eQTLs identified in all species are local eQTLs [32]. The SNPs of Target X associated with T2DM have been identified as cis-eQTLs linked to upregulation of Target X expression.

## 3.7 Cell lines

### 3.7.1 EndoC- $\beta$ H1 cells

The impact of upregulating Target X on pancreatic  $\beta$ -cells was in this project studied in a human pancreatic  $\beta$ -cell line, EndoC- $\beta$ H1. The cell line has been generated from human fetal pancreases and the cells express many genes and markers, such as transcription factors, that are  $\beta$  cell-specific [33]. Further, expression of markers that are specific to other pancreatic cell types have not been found at significant levels in EndoC- $\beta$ H1. The insulin content in these cells is stable over passages and stimulation with glucose induces insulin secretion [33].

### 3.7.2 MIN6 cells

Functional analysis of Target X was also performed in experimental work with a mouse pancreatic  $\beta$ -cell line, MIN6. MIN6 is a mouse  $\beta$ -cell line established from  $\beta$ -cell tumors, insulinomas, in transgenic mice [34]. The cell line has been observed to have similar insulin secretion in response to glucose stimulation as islets with a six- to seven-fold increase in insulin secretion at 25 mM glucose compared to at 5 mM glucose [35]. MIN6 cells have a rapid uptake of glucose due to high expression levels of glucose transporter GLUT-2.  $V_{max}$  of GLUT-2 for glucose transport is greater than that of GLUT-1, which is the glucose transporter in human  $\beta$ -cells [35]. Studies of gene expression and hormone secretion of MIN6 cells have revealed that MIN6 is not a pure  $\beta$ -cell line, and that the cells predominantly produce insulin, but also other hormones of the other endocrine cell types in the islets such as glucagon, somatostatin and ghrelin [36].

## 3.8 Techniques & Functional assays

### 3.8.1 Adenoviral transduction

Overexpression of Target X was in this study achieved using an adenoviral vector. Adenoviruses are non-enveloped, double-stranded DNA viruses classified into 7 species (A-G) and further subdivided into more than 50 serotypes based on genetic analyses [37]. The various human serotypes have been associated with ability of infecting a range of tissues causing diseases such as respiratory disease, conjunctivitis, gastroenteritis and pharyngoconjunctival fever [38, 39]. Adenoviruses are commonly used as vectors for gene transfer in mammalian cells. Advantages of using adenoviruses as vectors include excellent transduction efficiency, ability to infect both dividing and non-dividing cells, easily manipulated genome and well-characterized biology and structure [40, 41]. Deletions of viral proteins in early regions of the viral genome eliminates self-replication of the adenovirus [40]. Transduction with adenovirus results in a transient gene expression in the host cell [42].

### 3.8.2 Quantitative real-time PCR

Quantitative real-time Polymerase Chain Reaction (qPCR) is a widely used technology that has become the method of choice for detection of mRNA levels. In contrast to PCR, qPCR is quantitative and allows for real-time detection of the concentration of amplified DNA in the sample of each of the PCR cycles. To detect the mRNA expression levels with qPCR, the mRNA needs to be reverse transcribed into cDNA [43]. Detection of the amplified DNA is enabled by labeling it with a fluorescent reporter probe or a DNA binding dye. The probes used in this study are labeled with a non-fluorescent quencher and a minor groove binder (MGB) at the 3' end. The MGB component increases the melting temperature and hybridization specificity of the probe [44]. At the 5' end the probe is labeled with a fluorogenic reporter dye, 6-Carboxyfluorescein (FAM<sup>TM</sup>). The fluorescence from the reporter fluorochrome is suppressed by the close proximity to the quencher by fluorescence energy transfer (FRET). After hybridization of the probe to its complementary DNA, it is degraded by the Taq polymerase during extension of the DNA, releasing the fluorogenic reporter from the probe and from the quencher. This results in fluorescence emitted from the reporter fluorochrome that can be detected [45].

The amount of fluorescent signal that is detected during the amplification is directly proportional to the DNA in the sample prior to the PCR process. When the detected amount of fluorescence reaches an assigned threshold, that PCR cycle is assigned the threshold cycle ( $C_T$ ). The  $C_T$  value is set at a level where the PCR amplification is in the exponential phase and it is inversely related to the initial concentration of the cDNA template (*i.e.* the higher  $C_T$ , the lower amount of initial cDNA template) [43]. To enable comparison between samples, mRNA levels are normalized to measured levels of an internal reference gene. The expression levels of that gene is assumed to be stable in different experimental treatments [46]. In this project samples are normalized to glyceraldehyde-3-phosphate dehydrogenase (GAPDH) which is commonly used as a reference gene in qPCR. The relative gene expression is obtained using  $\Delta\Delta C_T$  -method. The  $C_T$  values of the genes are subtracted by the  $C_T$  values of the reference gene and a  $\Delta C_T$  value is created, see equation 3.1. Next, a  $\Delta\Delta C_T$  value is obtained by subtracting the  $\Delta C_T$  values of the samples with the  $\Delta C_T$  value of a reference gene, see equation 3.2. By calculating  $2$  to the power of  $-\Delta\Delta C_T$ , the relative expression of each gene is obtained, see equation 3.3, with the relative expression of the reference sample set to 1 [47].

$$\Delta C_T = C_{T(gene)} - C_{T(reference)} \quad (3.1)$$

$$\Delta\Delta C_T = \Delta C_{T(gene)} - \Delta C_{T(reference)} \quad (3.2)$$

$$2^{-\Delta\Delta C_T} \quad (3.3)$$

### 3.8.3 Homogeneous Time-Resolved Fluorescence

Homogeneous Time-Resolved Fluorescence (HTRF) is an immunoassay developed by Cisbio Bioassays [48]. HTRF immunoassay is used in this study in the glucose stimulated insulin secretion (GSIS) assay to measure the amount of insulin secreted. The technology is a combination of time resolved measurement and FRET technology. The FRET phenomena can be detected with unbound components in the sample, consequently there is no need for further separation or washing steps in HTRF assays. Time-resolved measurements eliminates short-lived background noise from e.g. buffers or proteins, by introducing a time-delay between excitation and measurement. Since the fluorescence emitted from the acceptor is long-lived, the FRET signal will thus still be detected [48]. In HTRF immunoassay, there are different donor-acceptor pairs of fluorophores that can be used. In the GSIS assay, the donor, Europium cryptate ( $\text{Eu}^{3+}$  cryptate), is a complex of a lanthide ion, Europium, embedded in a cyclic macromolecule, a trisbipyridine motif. The structure of the complex is the key behind the long-lived fluorescence in HTRF. A pigment purified from red algae, XL655, is the acceptor. Both the acceptor and donor are bound to a monoclonal antibody specific to insulin. When the pair is at close proximity, fluorescence can be detected at a wavelength of 665nm [48].

### 3.8.4 Apoptosis Assay

Apoptosis, or programmed cell death, is a highly conserved mechanism essential for cellular homeostasis and maintenance of cell number in tissues of multicellular organisms. The mechanisms of apoptosis are highly regulated and complex, and regulatory failure or impairment can cause e.g. neurodegenerative diseases, defects or cancer [49]. As previously has been described, T2DM is characterized by a decrease in total  $\beta$ -cell mass and increased frequency of  $\beta$ -cell apoptosis [3]. To address whether Target X impacts apoptosis in  $\beta$ -cells, apoptosis was stimulated in an assay measuring the activity of caspase 3 and 7. Both these members of the cysteine aspartic acid-specific protease (caspase) family are involved in the coordination of apoptosis in mammalian cells [50]. The Caspase-Glo® 3/7 Assay (Promega) [51], is based on detection of luminescence revealing the amount of caspase 3 and 7 activity in the sample. A caspase 3/7 specific luminogenic substrate, Z-DEVD-aminoluciferin, is added to the cells. Induction of apoptosis results in cleavage of the substrate by caspase 3/7 and release of aminoluciferin, a luciferase substrate. Reaction between the luciferase and aminoluciferin generates a luminescent light that can be measured. The luminescent signal is proportional to caspase 3/7 activity [52]. Three types of apoptosis inducers, tunicamycin, thapsigargin and a cytokine mixture, are used to stimulate apoptosis in the caspase 3/7 assay. Tunicamycin is a N-glycosylation inhibitor blocking the synthesis of N-linked oligosaccharides in the endoplasmic reticulum (ER) [53]. Further, tunicamycin promotes ER stress and induces apoptosis by disruption of protein folding in ER [54]. Thapsigargin inhibits ATP-dependent  $\text{Ca}^{2+}$ -pumps in ER leading to depletion of internal ER  $\text{Ca}^{2+}$  stores, accumulation of unfolded proteins and ER stress [55]. The mixture of cytokines consists of interleukin-1 $\beta$  (IL-1 $\beta$ ), tumor necrosis factor alpha (TNF- $\alpha$ ) and interferon- $\gamma$  (IFN- $\gamma$ ).

#### 3.8.5 Proliferation assay

Impact of Target X on the proliferative capacity of  $\beta$ -cells was in this study evaluated in a proliferation assay. Proliferating cells are detected by addition of 5-ethynyl-2-deoxyuridine (EdU), a thymidine analogue in which the methyl group has been replaced with an alkyne group. EdU can be incorporated into DNA synthesized in dividing cells during S-phase. Detection is achieved through the covalently binding of a fluorescent azide to the alkyne group in EdU. Thus, labeling dividing cells and allowing them to be detected by imaging [56]. Nuclei of all cells are stained with a Nuclear Blue stain. Proliferation was assessed in response to two stimuli; glucose and 1-azakenpauillone (1-AKP), which is an inhibitor of Glycogen synthase kinase-3 (GSK3) [57]. GSK3 is a regulator in the insulin signaling pathway and has been shown to be a negative regulator of  $\beta$ -cell proliferation [58]. Further, inhibition of GSK3 has been revealed to stimulate proliferation of pancreatic  $\beta$ -cells [57].

# 4

## Materials & Methods

This section describes the cell culturing of EndoC- $\beta$ H1 and MIN6 cells. Furthermore, the methods of the functional assays and analyses performed are outlined as well as the materials used. In statistical analysis of generated data, only p-values  $\leq 0.05$  were considered significant.

### 4.1 Cell culture: EndoC- $\beta$ H1

EndoC- $\beta$ H1 cells were maintained at 37°C and 5% CO<sub>2</sub> in DMEM (5.5 mM glucose) supplemented with 0.01%  $\beta$ -mercaptoethanol, 10 mM Nicotinamide, 1% Penicillin-Streptomycin, 2% Fatty acid free albumin from bovine serum (BSA) fraction, 5.5  $\mu$ g/mL Transferrin and 0.001% Sodium selenite. Cells were passaged once a week. For further information of EndoC- $\beta$ H1 culturing, see appendix A.

### 4.2 Cell culture: MIN6

MIN6 cells were maintained at 37°C and 5% CO<sub>2</sub> in DMEM (25 mM glucose) supplemented with 10% fetal bovine serum (FBS), 1% Penicillin-Streptomycin and 50  $\mu$ M  $\beta$ -mercaptoethanol. Medium was changed every third day and cells were passaged when 70-80% confluent. For further information of MIN6 cell culturing, see appendix B.

### 4.3 Adenoviral vectors

Adenoviral vectors were premade by Vigene Biosciences, derived from adenovirus type 5 and with two early regions, E1 and E3, deleted. The first vector contained the open reading frame (ORF) of Target X with a C-terminal Flag-HIS tag, and the second vector, serving as a control, contained an ORF encoding green fluorescent protein (GFP). The ORFs have been cloned into an adenoviral vector backbone, pAD, and are under regulation by a strong cytomegalovirus (CMV) promoter, see appendix D, figure D.1.

## 4.4 Selection of adenoviral concentration for over-expression

### 4.4.1 RNA extraction

Cells were seeded in a 96-well plate at a final concentration of  $50 \times 10^3$  cells/well in 100  $\mu$ L culture media. For EndoC- $\beta$ H1 cells the wells were coated with fibronectin and ECM. The plate was incubated overnight at 37°C. Cells were transduced with adenovirus containing vector with GFP or Target X in a range of MOIs (multiplicity of infection) (0-1000 for EndoC- $\beta$ H1 and 0-500 for MIN6). The plate was incubated at 37°C and culture media was changed after 24 hours. RNA was extracted using RNeasy Mini® kit (Qiagen®). After 72 hours, cells were lysed according to instructions in manufacturer’s protocol of RNeasy Mini® kit (Qiagen®). Samples were diluted at a 1:2 ratio with ethanol. To extract RNA, instructions according to manual were followed and optional DNase digestion steps were included.

### 4.4.2 Quantitative PCR (qPCR)

Quantitative PCR was used to evaluate the mRNA levels of Target X in EndoC- $\beta$ H1 cells and MIN6 cells transduced with adenovirus in a range of MOIs (0-1000 for EndoC- $\beta$ H1 and 0-500 for MIN6). RNA was extracted using RNeasy Mini® kit (Qiagen®) as previously outlined. Concentration of RNA was measured using NanoDrop to an average concentration of 10 ng/ $\mu$ L. Due to low concentration of RNA, 14.2  $\mu$ L of each sample was used in the DNA synthesis instead of 10  $\mu$ L as instructed in protocol. To each sample, 2  $\mu$ L 10xRT Buffer, 0.8  $\mu$ L 125xdNTP MIX (100 mM), 2  $\mu$ L 10xRT Random Primers and 1  $\mu$ L Multiscribe<sup>TM</sup> Reverse Transcriptase was added to a total volume of 20  $\mu$ L. The plate was sealed followed by a brief centrifugation to avoid air bubbles and to spin down contents. Reactions were loaded in a thermal cycler and the program in table 4.1 was run.

**Table 4.1:** Reverse transcription program scheme.

Step	Temperature (°C)	Time
Incubation	25.0	10 min.
Reverse transcription	37.0	2.00 hr.
Inactivation of reverse transcriptase	85	5 min.
Cooling	4	$\infty$

The cDNA synthesized was used as a template in qPCR. TaqMan® probes were ordered from and premade by Thermofisher. Gene evaluation was done for Target X and a housekeeping gene, glyceraldehyde-3-phosphate dehydrogenase (GAPDH/-Gapdh). Since two splice variants of Target X exists, a TaqMan® probe with best coverage was used to ensure detection of both variants. Samples were diluted to 5 ng/ $\mu$ L with DNase- & RNase-free H<sub>2</sub>O. Next, 2  $\mu$ L sample was mixed with 5  $\mu$ L TaqMan® Gene Expression Master Mix (Thermofisher), 2.5  $\mu$ L RNase-free H<sub>2</sub>O and 0.5  $\mu$ L TaqMan® probe to a total volume of 10  $\mu$ L. PCR was run in Quantstudio<sup>TM</sup>

7 Flex Real-Time PCR system according to the scheme in table 4.2. Comparative  $C_T$  method was used to obtain relative gene expression of Target X. Measured values of Target X were normalized to measured levels of GAPDH or Gapdh.

**Table 4.2:** qPCR program scheme.

Temperature (°C)	Time	Number of cycles
50.0	2 min	1
95.0	10 min	1
95.0	15 sec	} 40
60.0	1 min	

## 4.5 Apoptosis Assay

Apoptosis was evaluated when induced by tunicamycin, thapsigargin and a mixture of cytokines (IL- $\beta$ , TNF- $\alpha$ , IFN- $\gamma$ ) using Caspase-Glo® 3/7 Assay (Promega). Cells were seeded in a 96-well plate at a final concentration of  $50 \times 10^3$  (EndoC- $\beta$ H1) and  $30 \times 10^3$  (MIN6) cells/well in 100  $\mu$ L culture media. For EndoC- $\beta$ H1 cells the wells were coated with fibronectin and ECM. The plate was incubated overnight at 37°C. Cells were transduced with adenovirus diluted in culture medium at final concentrations of MOI 50 and MOI 200. The plate was incubated 24 hours at 37°C. Media was replaced by 100  $\mu$ L culture media and the plate was incubated at 37°C overnight. Dilutions with culture medium of apoptosis inducers were prepared to final concentrations of: 15  $\mu$ g/mL tunicamycin, 2  $\mu$ M thapsigargin and cytokine mixture (IFN- $\gamma$  40 ng/mL, IL-1 $\beta$  20 ng/mL, TNF- $\alpha$  40 ng/mL). DMSO (1:1000) was added to control since stock solutions of inducers were dissolved in DMSO. Media was replaced by 100  $\mu$ L reagent media and the plate was incubated at 37°C overnight. The next morning Caspase-Glo® Substrate was mixed with Caspase-Glo® Buffer (2.5 mL) resulting in Caspase-Glo® reagent. To each well, 100  $\mu$ L reagent was added and the plate was incubated at room temperature for 45 minutes. Luminescence was read in PHERAstar FS® plate reader and data was analyzed in GraphPad Prism 7. Statistical significance was determined using two-way ANOVA followed by Sidak's multiple comparisons test using Prism analysis program (GraphPad Prism 7).

## 4.6 Glucose Stimulated Insulin Secretion Assay

Cells were seeded in a 96-well plate at a final concentration of  $50 \times 10^3$  cells/well in 100  $\mu$ L culture media. For EndoC- $\beta$ H1 cells the wells were coated with fibronectin and ECM. The plate was incubated overnight at 37°C. Cells were transduced with diluted adenovirus at final concentrations of MOI 50 or MOI 200. The plate was incubated 24 hours at 37°C. Media was replaced by 100  $\mu$ L/well culture media. The plate was incubated at 37°C overnight. For EndoC- $\beta$ H1 cells media was replaced by 100  $\mu$ L/well culture medium (2.8 mM glucose) to starve the cells the day before the assay. The glucose starvation reduces variations in basal insulin secretion between cells. The plate was incubated at 37°C overnight. At the day of the assay, media

was replaced by 100  $\mu$ L Krebs buffer (100  $\mu$ L Krebs-Ringer buffer,  $\text{CaCl}_2$  1.007 mM, BSA fraction 0.2%, Glucose 0.5 mM) for EndoC- $\beta$ H1 cells. With MIN6 cells, media was replaced with 200  $\mu$ L glucose-free Krebs buffer (200  $\mu$ L Krebs-Ringer buffer,  $\text{CaCl}_2$  2.5 mM, BSA fraction 0.10%). The plate was incubated at 37°C, 1 hour. For Krebs-Ringer Buffer preparation, see appendix C, tables C.1 and C.2. Media was then replaced by 100  $\mu$ L low glucose Krebs buffer (100  $\mu$ L Krebs-Ringer buffer,  $\text{CaCl}_2$  1.007 mM, BSA fraction 0.2%, Glucose 2.8 mM, 0.5 mM IBMX) or 100  $\mu$ L high glucose Krebs buffer (100  $\mu$ L Krebs-Ringer buffer,  $\text{CaCl}_2$  1.007 mM, BSA fraction 0.2%, Glucose 16.7 mM, 0.5 mM IBMX). With MIN6 cells, media was replaced with 200  $\mu$ L low glucose Krebs buffer (200  $\mu$ L Krebs-Ringer buffer,  $\text{CaCl}_2$  2.5 mM, BSA fraction 0.10%, Glucose 2.8 mM) or 200  $\mu$ L high glucose Krebs buffer (200  $\mu$ L Krebs-Ringer buffer,  $\text{CaCl}_2$  2.5 mM, BSA fraction 0.10%, Glucose 16.7 mM). The plate was incubated at 37°C, 1 hour before 60  $\mu$ L/sample was transferred to a new 96-well plate and centrifuged at 4°C (3000 rpm, 5 min). To ensure that only supernatant and no cells were collected, 40  $\mu$ L/sample was collected from top of sample volume and transferred to a new 96-well plate.

Amount of insulin secreted was quantified using Insulin Sensitive Kit (Cisbio Assays). An insulin standard curve was prepared in the range 10-0.312 ng/mL. Samples were diluted with Krebs buffer (100  $\mu$ L Krebs-Ringer buffer,  $\text{CaCl}_2$  1.007 mM, BSA fraction 0.2%, Glucose 0.5 mM). Stock solutions with antibodies bound to XL655 and Cryptate were diluted 1:40 in Reconstitution Buffer (50 mM phosphate buffer, pH 7.0). Reagents were added to a black walled 384-well plate in the following order; 10  $\mu$ L sample or insulin standard, 5  $\mu$ L anti-insulin Ab-cryptate and last 5  $\mu$ L anti-insulin Ab-XL655. Plate was covered with a black plate film and incubated for 2 hours at room temperature. Homogenous time-resolved fluorescence was read in PHERAstar FS® plate reader. Insulin levels were determined by interpolating measured fluorescence intensity of samples to insulin standard curve using linear regression in Prism analysis program (GraphPad Prism 7).

## 4.7 Proliferation assay

Proliferation when overexpressing Target X was evaluated using Click-iT® EdU HCS Assay (Invitrogen).

### 4.7.1 EndoC- $\beta$ H1 cells

Cells were seeded in a black walled 96-well plate coated with ECM and fibronectin at a final concentration of  $50 \times 10^3$  cells/well in 100  $\mu$ L culture media followed by incubation at 37°C for two days. Cells were transduced with adenovirus, MOI 50 and MOI 200, containing GFP or Target X and were incubated at 37°C for two days. In order to synchronize the proliferation between cells, media was replaced with 100  $\mu$ L culture media containing 0.5 mM glucose, see appendix A, table A.2. Cells were incubated at 37°C for 6 hours. Media was replaced with 100  $\mu$ L of either 2.8 mM Glucose culture media (DMSO 1:1333), 2.8 mM Glucose Culture media (15  $\mu$ M 1-AKP in DMSO) or 5.5 mM Glucose culture media and cells were incubated at 37°C

for three days. EdU was diluted in respective culture media and 50  $\mu\text{L}$  was added to each well obtaining a final concentration of 10  $\mu\text{M}$ . Cells were incubated at 37°C for 4 hours. Media was removed and 100  $\mu\text{L}$  3.7% methanol-free formaldehyde in PBS was added to fix the cells, followed by 15 min incubation at room temperature. Fixative was removed and cells were washed twice with PBS. To permeabilize the cells, 100  $\mu\text{L}$  of 0.1% Triton® X-100 in PBS was added to each well followed by incubation 15 min at room temperature. Permeabilization buffer was removed followed by washing with PBS twice. To each sample, 80  $\mu\text{L}$  Click-iT® reaction cocktail (69  $\mu\text{L}$  Click-iT® EdU reaction buffer, 3.2  $\mu\text{L}$   $\text{CuSO}_4$ , 0.2  $\mu\text{L}$  Alexa Fluor®647 azide, 8  $\mu\text{L}$  Click-iT® EdU buffer additive (diluted 1:10 in deionized  $\text{H}_2\text{O}$ )) was added followed by incubation for 30 min at room temperature protected from light. HCS NuclearMask<sup>TM</sup> Blue stain was diluted 1:2000 in PBS. Click-iT® reaction cocktail was removed and 100  $\mu\text{L}$  diluted HCS NuclearMask<sup>TM</sup> Blue stain solution was added to each well to stain nuclei, followed by 30 min incubation at room temperature protected from light. The HCS NuclearMask<sup>TM</sup> Blue stain was removed followed by two washing steps with PBS. PBS was added to all wells and plate read by imaging in ImageXpress Micro. Images were analyzed and data was generated using MetaXpress® image analysis software. Data was further analyzed in GraphPad Prism 7. Statistical significance was determined by using one-way ANOVA followed by Tukey's multiple comparisons test using Prism analysis program (GraphPad Prism 7).

#### 4.7.2 MIN6 cells

MIN6 cells were incubated in two different mediums (with BSA or with FBS) to evaluate how these treatments affected proliferation. Cells were seeded in a black walled 96-well plate at a final concentration of  $20 \times 10^3$  cells/well in 100  $\mu\text{L}$  culture media. Cells were incubated at 37°C for two days before being transduced with adenovirus, MOI 200 and MOI 500, containing GFP or Target X. Cells were incubated at 37°C for two days. Media was replaced with 100  $\mu\text{L}$  DMEM (2.5 mM glucose, 0.1% BSA fraction) and cells were starved for 18 hours in order to synchronize proliferation between cells. Cells were incubated at 37°C for 48 hours with either DMEM (1% BSA fraction) and glucose concentrations 2.5 mM, 12 mM or 25 mM, or DMEM (10% FBS) and glucose concentrations 2.5 mM, 12 mM or 25 mM. EdU was diluted in respective incubation media and 50  $\mu\text{L}$  was added to each well obtaining a final concentration of 10  $\mu\text{M}$ . Cells were incubated at 37°C for 2 hours. Assay was run and analysis was proceeded as outlined in section 4.7.1.



# 5

## Results & Discussion

In this section, generated results from the measurements with both EndoC- $\beta$ H1 cells and MIN6 cells are presented and discussed. In section 5.1 the results obtained in qPCR analyses leading to the determination of adenoviral concentrations to be used in the study are presented and discussed. Further, the results from the three functional assays are presented and discussed starting with the apoptosis assays presented in section 5.2, the proliferation assays in section 5.3 and the results from the GSIS assays in section 5.4. Last, the generated data is further compared and discussed in section 5.5.

### 5.1 Determination of adenoviral concentrations for overexpression of Target X

As the impact of Target X and its function in  $\beta$ -cells was examined in this study in response to an overexpression of the gene to simulate the state in T2DM, a first and important step was to determine the concentrations of adenovirus needed to reach a suitable level of overexpression. Previous to this study, the mRNA expression of Target X in EndoC- $\beta$ H1 cells and in human islets have been measured, see figure 2.2 (b). As seen, the mRNA expression of Target X is markedly lower in EndoC- $\beta$ H1 cells compared to in human islets. As it was desirable to mimic the conditions in healthy human islets as a control, and in T2DM to study the function of Target X in the disease state, it was feasible to use two concentrations of adenovirus to overexpress Target X in EndoC- $\beta$ H1. The concentrations chosen were based on a qPCR analysis performed, in which a range of MOIs (0-1000) were analysed, see figure 5.1 (a). The basal mRNA expression, expressed as  $\Delta C_T$ , of Target X/GAPDH in human islets was equal to 0.0025, see figure 2.2 (b). In the qPCR analysis seen in figure 5.1 (a), MOI 50 resulted in an mRNA expression of Target X similar to the basal expression levels in the human islets. Further, an overexpression of Target X that was elevated in comparison to the upregulation in expression in T2DM  $\beta$ -cells was of desire to enlarge and enable detection of the effect of overexpressing Target X. As can be observed in figure 2.2 (a), there is a 2-3 fold upregulation in mRNA expression in T2DM  $\beta$ -cells compared to healthy ones. Therefore, MOI 200 was chosen as the concentration of overexpression of Target X since MOI 200 resulted in a 5-fold increase in mRNA expression of Target X compared to basal expression levels in human islets, see figure 5.1 (a).

The function of Target X in  $\beta$ -cells was in this study also examined in a mouse  $\beta$ -cell line, MIN6. The basal expression level of Target X (mouse) in MIN6 was measured in a qPCR analysis. Cells were in the same analysis transduced with adenovirus in a range of MOIs (0-500), see figure 5.1 (b). As a 5-fold increase in expression of Target X (human) was used in the study with the EndoC- $\beta$ H1 cells compared to expression levels in the human islets, it was feasible to use the same fold change in expression with MIN6 cells compared to basal expression levels of Target X (mouse). As can be observed in figure 5.1 (b), MOI 200 resulted in an expression of Target X (human) approximately 5-fold larger than the expression of Target X (mouse). Hence, MOI 200 was decided to be used in the functional assays with MIN6 cells.

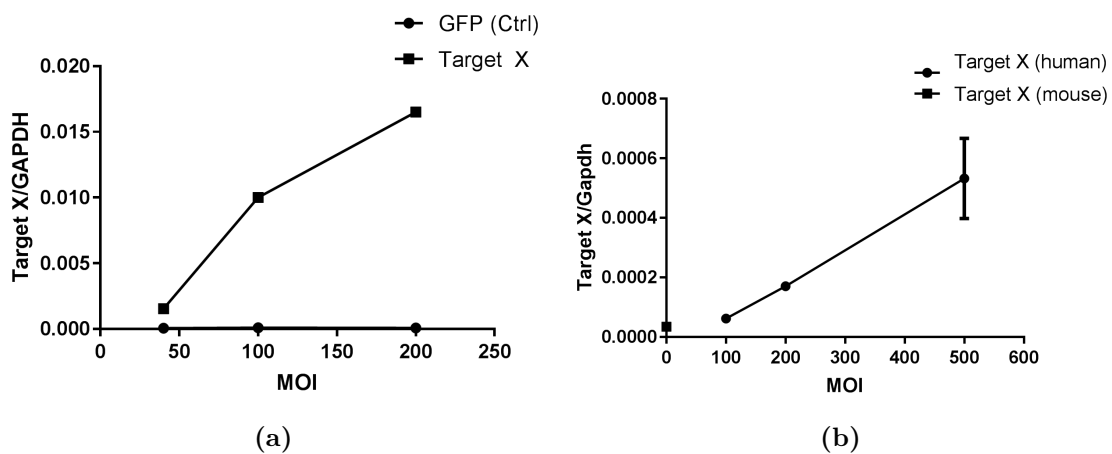
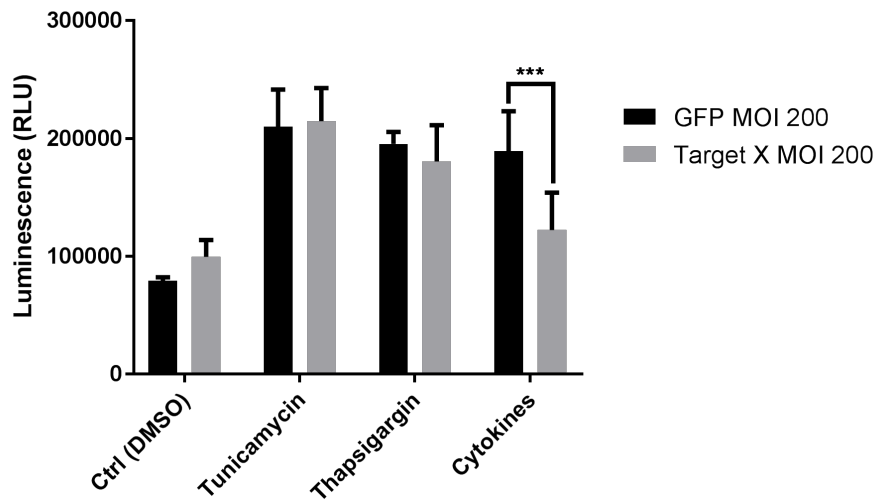


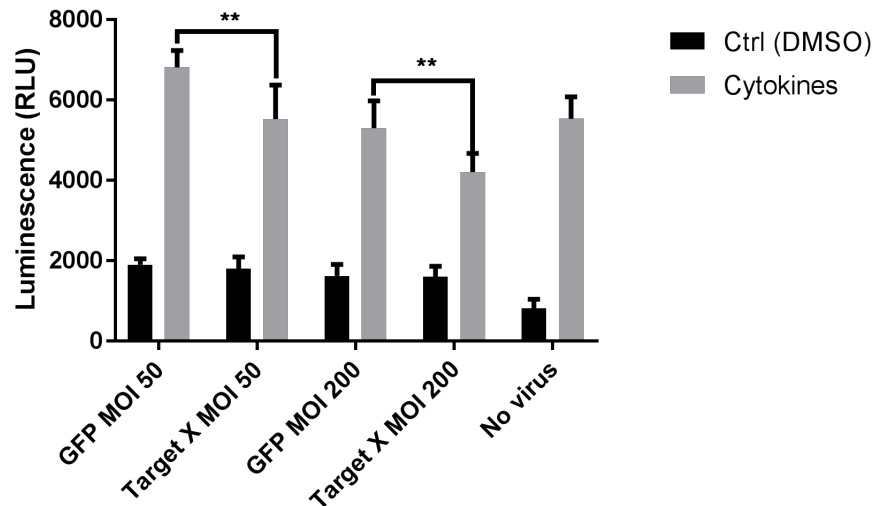
**Figure 5.1:** qPCR analysis of Target X mRNA expression. Values have been normalized to GAPDH or Gapdh and are displayed as calculated  $\Delta C_T$  values. Figure (a) displays mRNA expression of TargetX/GAPDH in EndoC- $\beta$ H1 cells transduced with either GFP vector (Ctrl) or vector containing Target X. Cells were transduced in a range of MOIs from 0-1000 (only MOIs 0-200 displayed). In figure (b) mRNA expression of Target X (mouse) in non-transduced samples are shown. The figure also displays the mRNA expression of Target X in samples transduced with Target X in a range of MOIs from 0-500. Error bars represents standard deviation.

## 5.2 Apoptosis assay

That a decrease in  $\beta$ -cell mass is central in the development of T2DM is supported by several studies [3, 21]. The main contributor to the decrease is generally assumed to be increased frequency of  $\beta$ -cell apoptosis [3]. There are several molecular mechanisms and pathways involved in and regulating mammalian apoptosis. To our knowledge, the role of Target X in  $\beta$ -cell apoptosis has prior to this project not been investigated. Hence, it was therefore unknown if Target X had a role in apoptosis and if so, in which mechanism regulating  $\beta$ -cell apoptosis it possibly was involved in. A screen was therefore completed with the EndoC- $\beta$ H1 cells with three inducers known to induce apoptosis in pancreatic  $\beta$ -cells but with different mechanisms, see figure 5.2 (a). All three inducers successfully induced apoptosis compared to control (DMSO). Interestingly, a significant reduction in apoptosis was seen when comparing overexpression with GFP (control virus) and Target X in apoptosis induced by cytokines (TNF- $\alpha$ , IFN- $\gamma$ , IL-1 $\beta$ ). This was unexpected as the genetic evidences suggests that an upregulation of Target X would have a detrimental impact on the biological function of  $\beta$ -cells. The experiment was repeated three times with only induction of apoptosis by the mixture of cytokines and with two MOIs. In all three experiments a significant reduction in apoptosis when overexpressing Target X compared to results with GFP was observed, see figure 5.2 (b). To address the possibility that the adenoviral transduction affected apoptosis, non-transduced samples (no virus) were included in the same measurement to enable a comparison to transduced ones. As seen in 5.2 (b), there is a small, but not significant, increase in apoptosis in transduced control (DMSO) samples compared to non-transduced control (DMSO) samples. The results implies that the transduction with adenovirus does not have a significant impact on apoptosis.



(a)



(b)

**Figure 5.2:** Caspase 3/7 activity measured by relative luminescence intensity in EndoC- $\beta$ H1 cells. In figure (a), apoptosis has been induced by tunicamycin (15  $\mu$ g/mL), thapsigargin (2  $\mu$ M) or a cytokine mixture (TNF- $\alpha$ , IFN- $\gamma$ , IL-1 $\beta$ ). Sample with DMSO serve as control. In figure (b), apoptosis has been induced by a cytokine mixture. Error bars represent standard deviation. \*\*\* denotes a significant level of  $p \leq 0.001$ , \* denotes a significant level of  $p \leq 0.005$ .

The impact of overexpressing Target X on apoptosis in  $\beta$ -cells was further examined in MIN6 cells. A screen with the same apoptosis inducers used in the apoptosis assay with EndoC- $\beta$ H1 was performed with the MIN6 cells as well. All three inducers successfully induced apoptosis compared to control (DMSO), see figure 5.3 (a). As seen, there is a suggested trend that overexpression of Target X possibly increase apoptosis in MIN6 cells compared to samples transduced with GFP. To further validate the significance of this trend, the assay was repeated with more replicates and with only tunicamycin as inducer. Tunicamycin was chosen as

inducer in the repeated apoptosis assay since that inducer appeared as the most efficient one in the first measurement, and returned a significant increase in apoptosis when overexpressing Target X. However, no significant difference in apoptosis could be observed in the repeated measurement, see figure 5.3 (b).

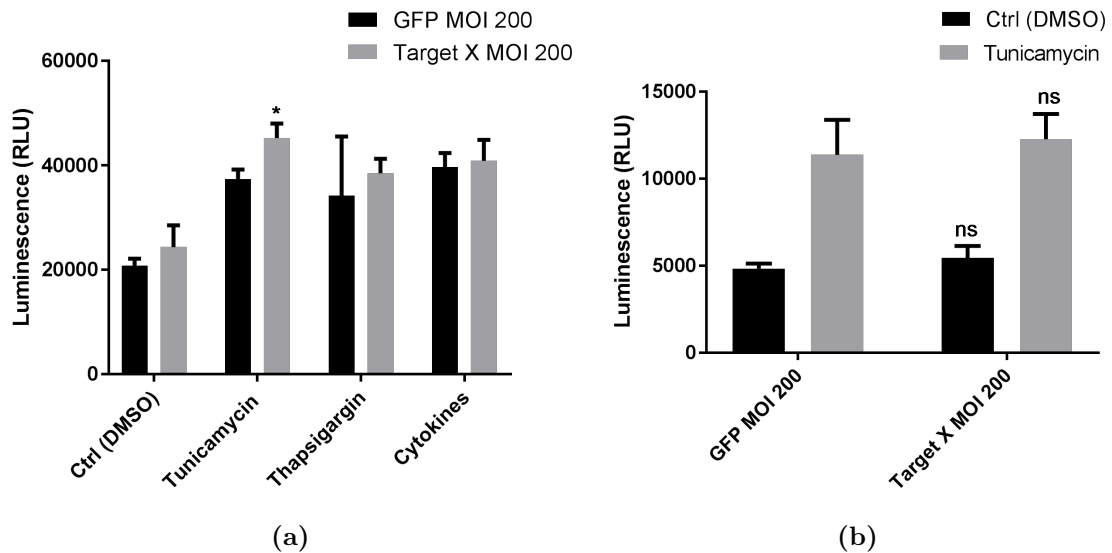


**Figure 5.3:** Measured caspase 3/7 activity by relative luminescence intensity in MIN6 cells transduced with GFP or Target X, MOI 200. In figure (a) apoptosis has been induced by addition of tunicamycin (15  $\mu\text{g}/\text{mL}$ ), thapsigargin (2  $\mu\text{M}$ ) or a cytokine mixture (TNF- $\alpha$ , IFN- $\gamma$ , IL-1 $\beta$ ). In figure (b), apoptosis has been induced by tunicamycin (15  $\mu\text{g}/\text{mL}$ ). Sample with DMSO serve as control. Error bars represent standard deviation. ns denotes not significant.

In addition, a separate qPCR analysis with samples from the apoptosis assay in figure 5.3 (b) was performed as a control of the mRNA expression of Target X in MIN6 cells, see figure 5.4. The mRNA expression of Target X (human) and Target X (mouse) was measured in samples transduced with MOI 200 and non-transduced samples. As seen, MOI 200 returned an mRNA expression of Target X (human) similar to the basal expression level of Target X (mouse). Consequently, the overexpression of Target X with MOI 200 in the performed apoptosis assay represents only a 2-fold increase in mRNA expression, and not a 5-fold increase. Further, the measured mRNA expression of Target X (mouse) is similar in non-transduced samples and samples transduced with MOI 200. Hence, it can be assumed that the transduction of MIN6 cells with Target X did not affect the gene expression of Target X (mouse).

The data from the apoptosis assays with EndoC- $\beta\text{H1}$  cells suggests that Target X has a protective role in apoptosis induced by cytokines, which is further not supported in the data generated in the apoptosis assays with MIN6 cells. Nevertheless, it should be taken into consideration that MOI 200 represents a 6-7 fold increase of Target X compared to basal expression levels in EndoC- $\beta\text{H1}$ , but only a 2-fold

increase in MIN6 cells compared to basal expression levels of Target X (mouse). Possibly, a repetition of the assay with increased MOI with MIN6 cells could have generated a significant increase in apoptosis when overexpressing Target X, but this remains to be further evaluated.

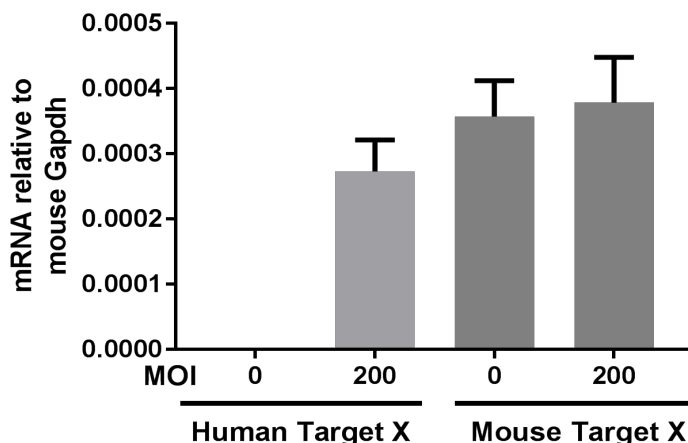


**Figure 5.4:** qPCR analysis of mRNA expression of Target X (human) and Target X (mouse) in non-transduced samples and in samples transduced with Target X MOI 200. Values have been normalized to Gapdh and are displayed as calculated  $\Delta C_T$  values. Error bars represent standard deviation.

### 5.3 Proliferation assay

The influence of overexpressing Target X on proliferation in  $\beta$ -cells was examined in an assay measuring DNA synthesis in dividing cells. A previously established protocol for a proliferation assay with EndoC- $\beta$ H1 cells was used and the cells were induced with 1-AKP, a known inducer of proliferation in  $\beta$ -cells, or 5.5 mM glucose. As displayed in figure 5.5, both inducers, 1-AKP and 5.5 mM glucose, successfully induced proliferation compared to non-induced samples. However, when comparing the results between samples transduced with GFP and Target X, no significant difference was observed. When the proliferation assay was performed with MIN6 cells, a range of glucose concentrations, 2.5-25 mM glucose, were used to induce proliferation. This, since proliferation of cells is known to be a glucose-dependent process. Secondly, cells were grown in media supplemented with either 10% fetal bovine serum (FBS) or 1% bovine serum albumin (BSA) to evaluate the impact of respective treatment on proliferation. A third factor evaluated was the impact of increased concentration, MOI 500, of adenovirus on proliferation. Not surprisingly, MIN6 cells cultured in media supplemented with 10% FBS had increased percentage of EdU incorporation compared to cells cultured in media supplemented with 1% BSA, see figure 5.6 (a) and (b). FBS consists of BSA, but also other nutritional and macromolecular factors that facilitates cell growth. Further, in both figure 5.6 (a) and (b) a dose-response trend can be seen between glucose concentration and proliferation in which proliferation increase with increased concentration of glucose.

In neither treatment nor with an increased MOI, a significant difference when overexpressing Target X on proliferation in MIN6 cells can be observed. The data of the impact of overexpressing Target X on proliferation in MIN6 cells is consistent with the data generated in the proliferation assay with EndoC- $\beta$ H1 cells suggesting that overexpressing Target X does not affect proliferation in  $\beta$ -cells.

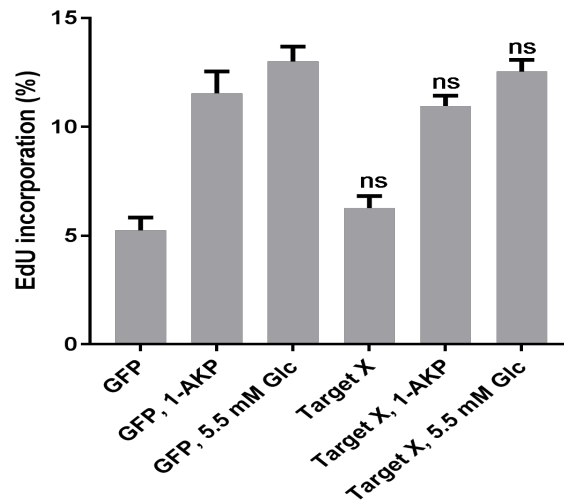


**Figure 5.5:** Displays the percentage of EdU incorporation in EndoC- $\beta$ H1 cells transduced with GFP or with Target X, MOI 200. Cells are treated with no inducer and 2.8 mM glucose, or with inducer: 1-AKP in 2.8 mM glucose or 5.5 mM glucose. Error bars represent standard deviation. ns denotes not significant.

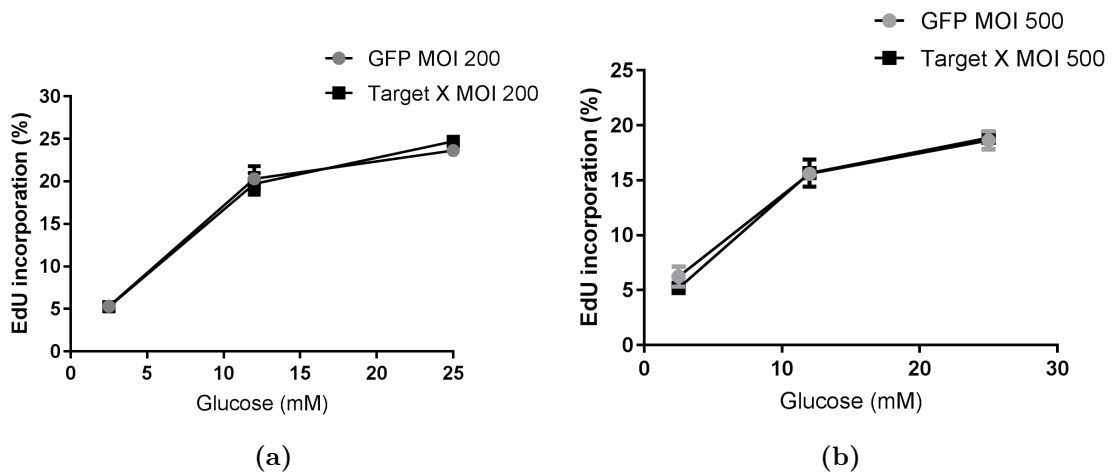


**Figure 5.6:** The percentage of EdU incorporation in MIN6 cells transduced with GFP or with Target X. Cells have been incubated 48 hours with a range of glucose concentrations of 2.5, 12, or 25 mM, with two different treatments and MOIs. In figure (a) cells have been incubated in DMEM containing 10% FBS, MOI 200, and in figure (b) DMEM containing 1% BSA, MOI 500.

## 5.4 Glucose stimulated insulin secretion assay

Insulin secretion by pancreatic  $\beta$ -cells in T2DM is insufficient to maintain blood glucose levels within a normal range, which gradually results in development of hyperglycemia [16]. The impact of overexpressing Target X on insulin secretion in  $\beta$ -cells was examined in a glucose stimulated insulin secretion (GSIS) assay. The amounts of insulin secreted (ng/mL) in response to low- or high concentration of glucose in EndoC- $\beta$ H1 cells are displayed in figure 5.7 (b). In a healthy  $\beta$ -cell, the insulin secreted when cells are stimulated with elevated glucose concentrations increase several folds in comparison to basal insulin secretion [59]. As can be seen in figure 5.7 (b), EndoC- $\beta$ H1 cells transduced with GFP MOI 50 have a high basal insulin secretion and low fold-response to GSIS. This is typical for EndoC- $\beta$ H1 cells and the data is consistent with a previous study by L. Andersson *et al.* [60], that have observed elevated basal insulin secretion and a low fold-response to GSIS in EndoC- $\beta$ H1 cells. Surprisingly, when Target X is overexpressed, a significant increase in fold-response to GSIS can be observed both at MOI 50 and MOI 200 compared to samples with GFP, see figure 5.7 (a). When cells are transduced with Target X MOI 50, the increase in fold-response is mainly a result of suppressed basal insulin secretion in comparison to samples transduced with GFP MOI 50, see figure 5.7 (b). With Target X MOI 200, the increase in fold-response is mainly caused by increased insulin secretion in response to stimulation with 16.7 mM glucose compared to samples transduced with GFP MOI 200. In T2DM patients, a decrease in fold-response in GSIS compared to healthy control is commonly observed. Further, the basal insulin secretion in response to low concentration of glucose is usually enhanced compared to controls [61]. Since an upregulated expression of Target X is associated with T2DM, a significant increase in fold-response to GSIS in correlation with an overexpression of Target X was unexpected results. The results from the GSIS assay with EndoC- $\beta$ H1 cells suggest a positive impact of Target X upregulation on insulin secretion in  $\beta$ -cells.

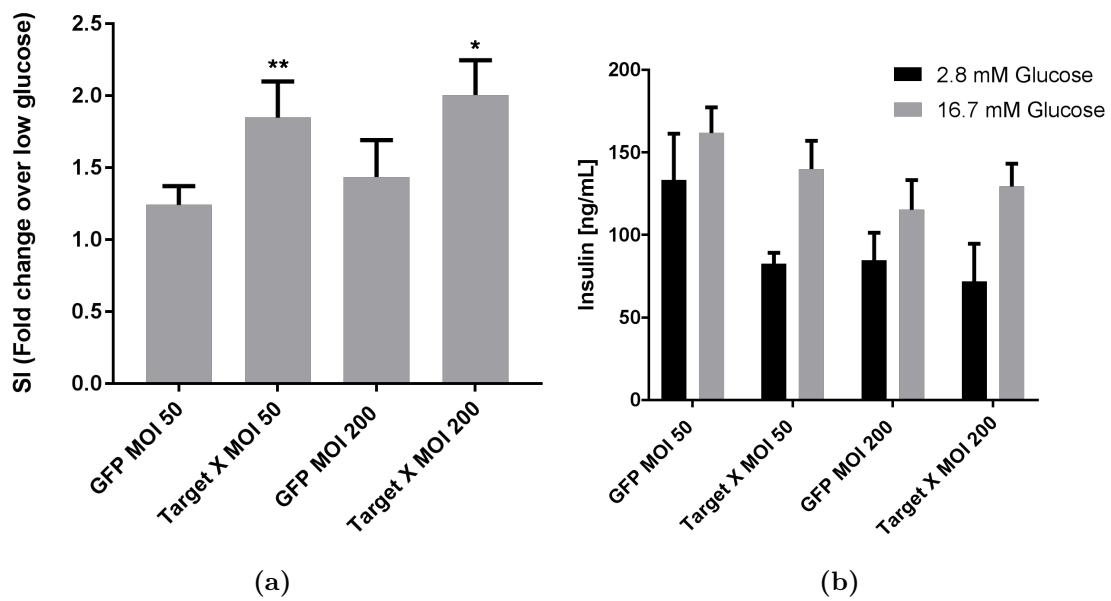


**Figure 5.7:** Insulin secreted (ng/mL) from EndoC- $\beta$ H1 cells transduced with either GFP or Target X and stimulated with either 2.8 mM glucose or 16.7 mM glucose. In figure (a), the Stimulation Index (SI) for each sample is displayed as the fold change over low glucose. In figure (b), the individual data for each sample is shown. Error bars represent standard deviation. \*\* denotes a significant level of  $p \leq 0.01$ , \* denotes a significant level of  $p \leq 0.05$ .

As previously has been described, MIN6 cells have similar insulin secretion in response to stimulation by glucose as islets [35]. This was consistent with the results from the GSIS assay in the present study with MIN6-cells seen in figure 5.8 (b). As seen in the figure, a low basal insulin secretion and a several fold increase in insulin secretion in response to glucose stimulation was observed, which is the typical pattern of insulin secretion by healthy  $\beta$ -cells [59]. Contrary to the data generated in the GSIS assay with EndoC- $\beta$ H1, a significant decrease in fold-response to GSIS was observed with the MIN6 cells, see figure 5.8 (a). The results supports the hypothesis that an upregulation of Target X has a harmful impact on the function of pancreatic  $\beta$ -cells. The results are further also consistent with the observation of a markedly lower fold-response to GSIS in T2DM patients compared to healthy control [61]. As a variation in mRNA expression in the previous qPCR analyses had been observed, an individual qPCR analysis was done in addition to the GSIS assay with MIN6 cells. The results seen in figure 5.9 implies that MOI 200 used in the GSIS assay results in a 2-fold increase in mRNA expression, in consistency to the qPCR analysis discussed in section 5.2. Again, the mRNA expression of Target X (mouse) in non-transduced samples is similar to the expression level of Target X (mouse) in transduced samples, suggesting that transduction with Target X (human) do not impact Target X (mouse) mRNA expression. When comparing the results in this assay between the two cell lines, it should thereby be noted that a difference exists in folds of overexpression of Target X in the assays between them. The data generated in the GSIS assays with EndoC- $\beta$ H1 cells and MIN6 cells implies that Target X possibly has a functional role involved in insulin secretion in pancreatic  $\beta$ -cells. However, the data generated in the GSIS assays is inconsistent between the two cell lines.

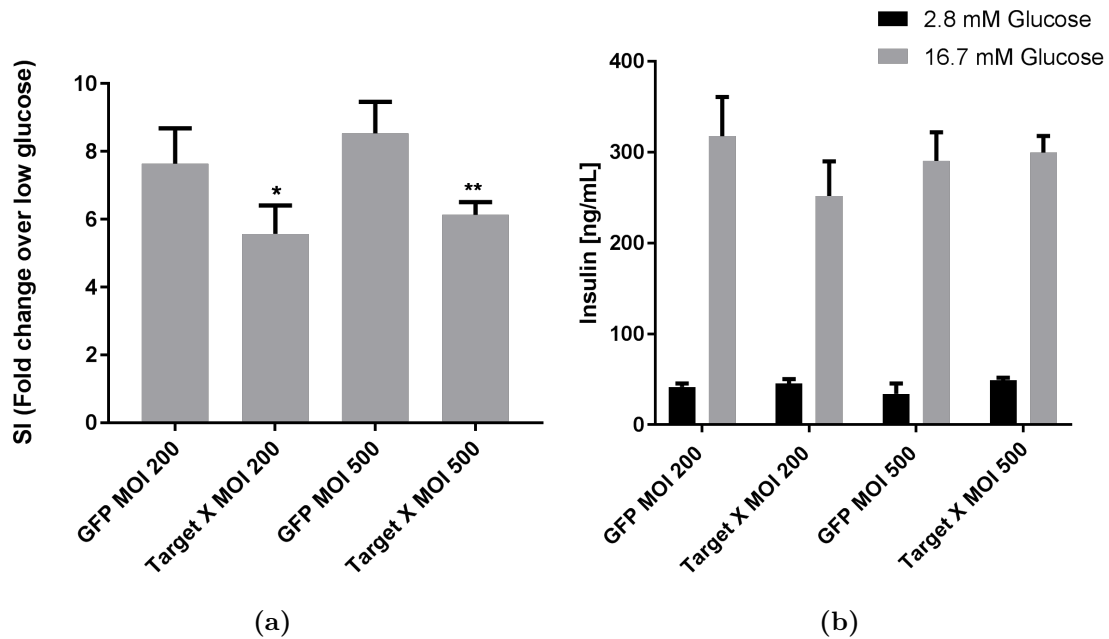


**Figure 5.8:** Insulin secreted (ng/mL) from MIN6 cells transduced with either GFP or Target X, MOI 200 or MOI 500, and stimulated with either 2.8 mM glucose or 16.7 mM glucose. In figure (a), the Stimulation Index (SI) for each sample is displayed as the fold change over low glucose. In figure (b), the individual data for each sample is shown. Error bars represent standard deviation. \*\* denotes a significant level of  $p \leq 0.01$ , \* denotes a significant level of  $p \leq 0.05$ .

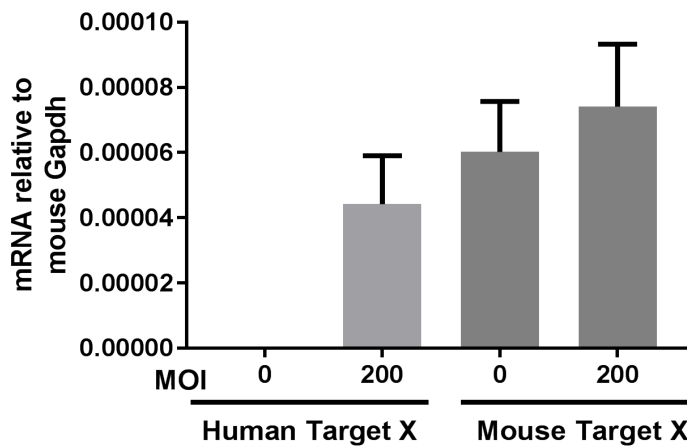


**Figure 5.9:** qPCR analysis of mRNA expression of Target X (human) and Target X (mouse) in non-transduced samples and in samples transduced with Target X MOI 200. Values have been normalized to Gapdh and are displayed as calculated  $\Delta C_T$  values. Error bars represent standard deviation.

## 5.5 Comparison of results with EndoC- $\beta$ H1 & MIN6

The results generated in the GSIS assay and the apoptosis assay with EndoC- $\beta$ H1 cells were somewhat unexpected and did not support the hypothesis that overexpression of Target X would have a deleterious effect on the function of  $\beta$ -cells. In contrast, the results suggests that overexpression of Target X possibly has a beneficial and protective influence on  $\beta$ -cell function. As previously has been described, the vector used in the adenoviral transduction in this study contained splice variant 1 of Target X. The decision to overexpress splice variant 1, and not splice variant 2, was based on a previous measurement of mRNA expression of Target X in healthy human islets in which splice variant 1 was observed to be more abundantly expressed, see figure 2.2 (b). Nevertheless, the expression levels of the two splice variants in human islets from T2DM donors have not been measured. Subsequently, there might be a difference in expression levels of the two splice variants between healthy islets and T2DM islets. It is possible, that there is an upregulation in gene expression of splice variant 2 in T2DM that has a detrimental impact on  $\beta$ -cell function in T2DM.

The decision to study the function of Target X in two  $\beta$ -cell lines was based on that the generated results with EndoC- $\beta$ H1 cells were not consistent with the genetic evidences. As described in section 5.1 and displayed in figure 2.2 (b), the mRNA expression of Target X in EndoC- $\beta$ H1 is very low compared to the expression in human islets. A possible consequence to consider is that the cell line might have some compensatory mechanisms for the lack of Target X. As a result, an overexpression of Target X would have minimal effect in a system that depends on other enzymes or pathways. Further, EndoC- $\beta$ H1 cells are grown in a serum-free culture medium without any addition of fatty acids. Since Target X is involved in lipid metabolism, an upregulation in gene expression of Target X might lead to depletion of substrate in the pathway Target X is involved in. This would result in a reduced effect of overexpressing Target X. Because of these two reasons, the decision was made to evaluate Target X in a second cell line, MIN6.

When comparing the results from the functional assays between the two cell lines, there are differences in the results between them. A possible reason is that differences exists in post-translational processing of the protein between the two cell lines, leading to an inefficient translation of Target X mRNA into functional protein in MIN6 cells. The main contributor to the differences seen in results is, however, probably the differences in folds of overexpression of Target X between the two cell lines. As has been mentioned, the fold increase in EndoC- $\beta$ H1 was 6-7 fold compared to basal mRNA expression levels of Target X in EndoC- $\beta$ H1, but the increase was only 2-fold in MIN6 cells compared to basal mRNA expression levels of Target X (mouse). According to the manufacturer of the adenoviral vector, the CMV promoter is functional in different mammalian cell types. Nevertheless, a high cell type variability in strength of the CMV promoter has been reported that could result in differences in gene expression between the two cell lines [62].

Variations observed in the results from the three qPCR analyses of mRNA expression of Target X in MIN6 cells could be a consequence of that the MIN6 cells used in the three measurements are from different batches. Hence, the expression levels of Target X might differ in between them. Further, even though the mRNA levels of Gapdh are assumed to be stable, the levels of genes defined as housekeeping genes have been reported to vary in different experimental conditions [63]. Differences between the measurements in levels of Gapdh can possibly have contributed to variations in the qPCR results.

# 6

## Conclusions & Outlook

### 6.1 Conclusions

Interestingly, overexpression of Target X in EndoC- $\beta$ H1 cells resulted in a reduction in apoptosis induced by cytokines. That an overexpression of Target X would have a protective influence in cytokine induced apoptosis was unexpected results, and not consistent with the hypothesis that upregulation of Target X would have a deleterious impact on  $\beta$ -cells. Further, overexpression of Target X significantly increased the fold-response to GSIS in EndoC- $\beta$ H1 cells. Again, this was surprising results since fold-response to GSIS is markedly lowered in T2DM patients.

Functional evaluation of Target X in MIN6 cells did not support the results generated with the EndoC- $\beta$ H1 cells. Instead, a small, but not significant, trend of increased apoptosis when overexpressing Target X was observed. Further, a significant decrease in fold-response to GSIS was observed when overexpressing Target X. The results from the apoptosis assay and GSIS assay with MIN6 cells supports the hypothesis of a harmful impact of Target X upregulation on pancreatic  $\beta$ -cells. No functional influence of Target X on  $\beta$ -cell proliferation in MIN6-cells nor in EndoC- $\beta$ H1 cells was observed. Nevertheless, that the overexpression of Target X in the functional assays with MIN6 cells only was 2-fold, is a factor to take into consideration when comparing the generated results between the two cell lines in this study. The results from the functional assays with EndoC- $\beta$ H1 cells and MIN6 cells suggests that upregulation of Target X expression may influence insulin secretion and apoptosis in pancreatic  $\beta$ -cells.

### 6.2 Outlook

Additional studies and experiments can further increase the understanding of the function of Target X, and the mechanism linking an upregulation of Target X to T2DM. It would be of interest to measure the mRNA expression of the two splice variants of Target X in T2DM islets to address the question whether there is a change in the expression levels of splice variant 1 and 2 in T2DM islets compared to healthy islets. It would further give an indication whether splice variant 2 might have a detrimental influence. By using specific probes for the two splice variants in a qPCR analysis with islets from T2DM donors, the mRNA levels can be measured. However, isolated islets from T2DM donors are of limited availability.

Measurement of the protein levels of Target X in the two cell lines would be of interest. In this study, only the mRNA expression has been evaluated. By measuring the protein levels of Target X, possibly by Western blot, it would be possible to determine the translational efficiency of Target X. In addition, a measurement of lipid intermediates in the pathway of Target X in transduced, and non-transduced samples would give an indication of the functionality of the protein.

This study has given a base for further analysis of the impact of Target X upregulation on pancreatic  $\beta$ -cells. Future studies and functional analyses with primary cells (*i.e.* human islets from cadaveric donors) would be valuable to get a greater understanding of the mechanism connecting T2DM and Target X upregulation.

Furthermore, if future functional analyses can demonstrate a harmful connection between an upregulation of Target X and T2DM, a next step would be to knock the gene expression of Target X. This could contribute to increased understanding of the functional role of Target X, and it would also simulate how an antagonistic drug targeting Target X would impact the  $\beta$ -cells. The gene expression could possibly be knocked by using siRNA.

# Bibliography

- [1] M. S. Islam, *The islets of langerhans*, vol. 654, pp. 19–21, 131–132, 709–170. Springer, 2010.
- [2] A. D. Association *et al.*, “Diagnosis and classification of diabetes mellitus,” *Diabetes care*, vol. 33, no. Supplement 1, pp. S62–S69, 2010.
- [3] A. E. Butler, J. Janson, S. Bonner-Weir, R. Ritzel, R. A. Rizza, and P. C. Butler, “ $\beta$ -cell deficit and increased  $\beta$ -cell apoptosis in humans with type 2 diabetes,” *Diabetes*, vol. 52, no. 1, pp. 102–110, 2003.
- [4] C. N. Rotimi, G. Chen, A. A. Adeyemo, P. Furbert-Harris, D. Guass, J. Zhou, K. Berg, O. Adegoke, A. Amoah, S. Owusu, *et al.*, “A genome-wide search for type 2 diabetes susceptibility genes in west africans,” *Diabetes*, vol. 53, no. 3, pp. 838–841, 2004.
- [5] A. A. Hardikar, *Pancreatic Islet Biology*, pp. 4–7. Springer, 2016.
- [6] S. Pandol, *The Exocrine Pancreas*, vol. 14, pp. 11–22. Morgan & Claypool Life Sciences, 2011.
- [7] R. A. DeFronzo, E. Ferrannini, P. Zimmet, and G. Alberti, *International Textbook of Diabetes Mellitus, 2 Volume Set*, vol. 1, pp. 56, 71. John Wiley & Sons, 2015.
- [8] A. Asakawa, A. Inui, H. Yuzuriha, N. Ueno, G. Katsuura, M. Fujimiya, M. A. Fujino, A. Niijima, M. M. Meguid, and M. Kasuga, “Characterization of the effects of pancreatic polypeptide in the regulation of energy balance,” *Gastroenterology*, vol. 124, no. 5, pp. 1325–1336, 2003.
- [9] L. Szablewski, *Glucose homeostasis and insulin resistance*, pp. 1, 46. Bentham Science Publishers, 2011.
- [10] J. E. Hall, *Guyton and Hall textbook of medical physiology*, pp. 986–989. Elsevier Health Sciences, 2015.
- [11] I. Quesada, M. G. Todorova, and B. Soria, “Different metabolic responses in  $\alpha$ -,  $\beta$ -, and  $\delta$ -cells of the islet of langerhans monitored by redox confocal microscopy,” *Biophysical journal*, vol. 90, no. 7, pp. 2641–2650, 2006.
- [12] M. E. Doyle and J. M. Egan, “Mechanisms of action of glucagon-like peptide 1 in the pancreas,” *Pharmacology & therapeutics*, vol. 113, no. 3, pp. 546–593, 2007.
- [13] P. E. Light, J. E. Manning Fox, M. J. Riedel, and M. B. Wheeler, “Glucagon-like peptide-1 inhibits pancreatic atp-sensitive potassium channels via a protein kinase a-and adp-dependent mechanism,” *Molecular Endocrinology*, vol. 16, no. 9, pp. 2135–2144, 2002.
- [14] F. M. Ashcroft and P. Rorsman, “Electrophysiology of the pancreatic  $\beta$ -cell,” *Progress in biophysics and molecular biology*, vol. 54, no. 2, pp. 87–143, 1989.

- [15] K. G. M. M. Alberti and P. f. Zimmet, “Definition, diagnosis and classification of diabetes mellitus and its complications. part 1: diagnosis and classification of diabetes mellitus. provisional report of a who consultation,” *Diabetic medicine*, vol. 15, no. 7, pp. 539–553, 1998.
- [16] S. E. Kahn, M. E. Cooper, and S. Del Prato, “Pathophysiology and treatment of type 2 diabetes: perspectives on the past, present, and future,” *The Lancet*, vol. 383, no. 9922, pp. 1068–1083, 2014.
- [17] F. B. Hu, J. E. Manson, M. J. Stampfer, G. Colditz, S. Liu, C. G. Solomon, and W. C. Willett, “Diet, lifestyle, and the risk of type 2 diabetes mellitus in women,” *New England journal of medicine*, vol. 345, no. 11, pp. 790–797, 2001.
- [18] D. P. P. R. Group *et al.*, “Reduction in the incidence of type 2 diabetes with lifestyle intervention or metformin,” *N Engl j Med*, vol. 2002, no. 346, pp. 393–403, 2002.
- [19] C. J. Nolan, P. Damm, and M. Prentki, “Type 2 diabetes across generations: from pathophysiology to prevention and management,” *The Lancet*, vol. 378, no. 9786, pp. 169–181, 2011.
- [20] L. Shi, G.-S. Tan, and K. Zhang, “Relationship of the serum crp level with the efficacy of metformin in the treatment of type 2 diabetes mellitus: A meta-analysis,” *Journal of clinical laboratory analysis*, vol. 30, no. 1, pp. 13–22, 2016.
- [21] J. Rahier, Y. Guiot, R. Goebbels, C. Sempoux, and J. Henquin, “Pancreatic  $\beta$ -cell mass in european subjects with type 2 diabetes,” *Diabetes, Obesity and Metabolism*, vol. 10, no. s4, pp. 32–42, 2008.
- [22] H. Sakuraba, H. Mizukami, N. Yagihashi, R. Wada, C. Hanyu, and S. Yagihashi, “Reduced beta-cell mass and expression of oxidative stress-related dna damage in the islet of japanese type ii diabetic patients,” *Diabetologia*, vol. 45, no. 1, pp. 85–96, 2002.
- [23] K. Maedler, J. Oberholzer, P. Bucher, G. A. Spinas, and M. Y. Donath, “Monounsaturated fatty acids prevent the deleterious effects of palmitate and high glucose on human pancreatic  $\beta$ -cell turnover and function,” *Diabetes*, vol. 52, no. 3, pp. 726–733, 2003.
- [24] D. Laybutt, A. Preston, M. Åkerfeldt, J. Kench, A. Busch, A. Biankin, and T. Biden, “Endoplasmic reticulum stress contributes to beta cell apoptosis in type 2 diabetes,” *Diabetologia*, vol. 50, no. 4, pp. 752–763, 2007.
- [25] G. Drews, P. Krippeit-Drews, and M. Düfer, “Oxidative stress and beta-cell dysfunction,” *Pflügers Archiv-European Journal of Physiology*, vol. 460, no. 4, pp. 703–718, 2010.
- [26] M. Masini, M. Bugliani, R. Lupi, S. Del Guerra, U. Boggi, F. Filipponi, L. Marselli, P. Masiello, and P. Marchetti, “Autophagy in human type 2 diabetes pancreatic beta cells,” *Diabetologia*, vol. 52, no. 6, pp. 1083–1086, 2009.
- [27] S. Del Guerra, R. Lupi, L. Marselli, M. Masini, M. Bugliani, S. Sbrana, S. Torri, M. Pollera, U. Boggi, F. Mosca, *et al.*, “Functional and molecular defects of pancreatic islets in human type 2 diabetes,” *Diabetes*, vol. 54, no. 3, pp. 727–735, 2005.
- [28] M. Anello, R. Lupi, D. Spampinato, S. Piro, M. Masini, U. Boggi, S. Del Prato, A. Rabuazzo, F. Purrello, and P. Marchetti, “Functional and morphological al-

- terations of mitochondria in pancreatic beta cells from type 2 diabetic patients,” *Diabetologia*, vol. 48, no. 2, pp. 282–289, 2005.
- [29] W. S. Bush and J. H. Moore, “Genome-wide association studies,” *PLoS Comput Biol*, vol. 8, no. 12, p. e1002822, 2012.
- [30] K. Appasani, *Genome-wide association studies: From polymorphism to personalized medicine*, pp. 139–141. Cambridge University Press, 2015.
- [31] T. A. Pearson and T. A. Manolio, “How to interpret a genome-wide association study,” *Jama*, vol. 299, no. 11, pp. 1335–1344, 2008.
- [32] F. W. Albert and L. Kruglyak, “The role of regulatory variation in complex traits and disease,” *Nature Reviews Genetics*, vol. 16, no. 4, pp. 197–212, 2015.
- [33] P. Ravassard, Y. Hazhouz, S. Pechberty, E. Bricout-Neveu, M. Armanet, P. Czernichow, and R. Scharfmann, “A genetically engineered human pancreatic  $\beta$  cell line exhibiting glucose-inducible insulin secretion,” *The Journal of clinical investigation*, vol. 121, no. 9, 2011.
- [34] J.-I. Miyazaki, K. Araki, E. Yamato, H. Ikegami, T. Asano, Y. Shibasaki, Y. Oka, and K.-I. YAMAMURA, “Establishment of a pancreatic  $\beta$  cell line that retains glucose-inducible insulin secretion: special reference to expression of glucose transporter isoforms,” *Endocrinology*, vol. 127, no. 1, pp. 126–132, 1990.
- [35] H. Ishihara, T. Asano, K. Tsukuda, H. Katagiri, K. Inukai, M. Anai, M. Kikuchi, Y. Yazaki, J. I. Miyazaki, and Y. Oka, “Pancreatic beta cell line min6 exhibits characteristics of glucose metabolism and glucose-stimulated insulin secretion similar to those of normal islets,” *Diabetologia*, vol. 36, no. 11, pp. 1139–1145, 1993.
- [36] K. Nakashima, Y. Kanda, Y. Hirokawa, F. Kawasaki, M. Matsuki, and K. Kaku, “Min6 is not a pure beta cell line but a mixed cell line with other pancreatic endocrine hormones,” *Endocrine journal*, vol. 56, no. 1, pp. 45–53, 2009.
- [37] S.-Y. Chang, C.-N. Lee, P.-H. Lin, H.-H. Huang, L.-Y. Chang, W. Ko, S.-F. Chang, P.-I. Lee, L.-M. Huang, and C.-L. Kao, “A community-derived outbreak of adenovirus type 3 in children in taiwan between 2004 and 2005,” *Journal of medical virology*, vol. 80, no. 1, pp. 102–112, 2008.
- [38] C. Rocholl, K. Gerber, J. Daly, A. T. Pavia, and C. L. Byington, “Adenoviral infections in children: the impact of rapid diagnosis,” *Pediatrics*, vol. 113, no. 1, pp. e51–e56, 2004.
- [39] P. W. Roelvink, A. Lizonova, J. G. Lee, Y. Li, J. M. Bergelson, R. W. Finberg, D. E. Brough, I. Kovesdi, and T. J. Wickham, “The coxsackievirus-adenovirus receptor protein can function as a cellular attachment protein for adenovirus serotypes from subgroups a, c, d, e, and f,” *Journal of virology*, vol. 72, no. 10, pp. 7909–7915, 1998.
- [40] A. Bett, L. Prevec, and F. Graham, “Packaging capacity and stability of human adenovirus type 5 vectors,” *Journal of virology*, vol. 67, no. 10, pp. 5911–5921, 1993.
- [41] N. Zhang, B. Schröppel, D. Chen, S. Fu, K. L. Hudkins, H. Zhang, B. M. Murphy, R. S. Sung, and J. S. Bromberg, “Adenovirus transduction induces expression of multiple chemokines and chemokine receptors in murine  $\beta$  cells

- and pancreatic islets,” *American Journal of Transplantation*, vol. 3, no. 10, pp. 1230–1241, 2003.
- [42] S. Knaän-Shanzer, I. Van Der Velde, M. J. Havenga, A. A. Lemckert, A. A. De Vries, and D. Valerio, “Highly efficient targeted transduction of undifferentiated human hematopoietic cells by adenoviral vectors displaying fiber knobs of subgroup b,” *Human gene therapy*, vol. 12, no. 16, pp. 1989–2005, 2001.
- [43] C. M. Taylor, R. Jost, W. Erskine, and M. N. Nelson, “Identifying stable reference genes for qrt-pcr normalisation in gene expression studies of narrow-leaved lupin (*lupinus angustifolius* l.),” *PLoS one*, vol. 11, no. 2, p. e0148300, 2016.
- [44] I. V. Kutyavin, I. A. Afonina, A. Mills, V. V. Gorn, E. A. Lukhtanov, E. S. Belousov, M. J. Singer, D. K. Walburger, S. G. Lokhov, A. A. Gall, *et al.*, “3′-minor groove binder-dna probes increase sequence specificity at pcr extension temperatures,” *Nucleic acids research*, vol. 28, no. 2, pp. 655–661, 2000.
- [45] R. E. Farrell, *RNA methodologies: a laboratory guide for isolation and characterization*, p. 528. Amsterdam: Elsevier/Academic Press, 2005.
- [46] J. Vandesompele, K. De Preter, F. Pattyn, B. Poppe, N. Van Roy, A. De Paepe, and F. Speleman, “Accurate normalization of real-time quantitative rt-pcr data by geometric averaging of multiple internal control genes,” *Genome biology*, vol. 3, no. 7, 2002.
- [47] J. Winer, C. K. S. Jung, I. Shackel, and P. M. Williams, “Development and validation of real-time quantitative reverse transcriptase–polymerase chain reaction for monitoring gene expression in cardiac myocytes in vitro,” *Analytical biochemistry*, vol. 270, no. 1, pp. 41–49, 1999.
- [48] L. Einhorn and K. Krapfenbauer, “Htrf: a technology tailored for biomarker determination—novel analytical detection system suitable for detection of specific autoimmune antibodies as biomarkers in nanogram level in different body fluids,” *EPMA Journal*, vol. 6, no. 1, p. 23, 2015.
- [49] J. J. Liu, W. Wang, D. T. Dicker, and W. S. El-Deiry, “Bioluminescent imaging of trail-induced apoptosis through detection of caspase activation following cleavage of devd-aminoluciferin,” *Cancer biology & therapy*, vol. 4, no. 8, pp. 885–892, 2005.
- [50] E. A. Slee, C. Adrain, and S. J. Martin, “Executioner caspase-3,-6, and-7 perform distinct, non-redundant roles during the demolition phase of apoptosis,” *Journal of biological Chemistry*, vol. 276, no. 10, pp. 7320–7326, 2001.
- [51] Promega Corporation, “Caspase-Glo® 3/7 Assay.” <https://se.promega.com/resources/protocols/technical-bulletins/101/caspase-glo-37-assay-protocol/>. Accessed: 2017-02-03.
- [52] M. Scabini, F. Stellari, P. Cappella, S. Rizzitano, G. Texido, and E. Pesenti, “In vivo imaging of early stage apoptosis by measuring real-time caspase-3/7 activation,” *Apoptosis*, vol. 16, no. 2, pp. 198–207, 2011.
- [53] Y.-H. Ling, T. Li, R. Perez-Soler, and M. Haigentz, “Activation of er stress and inhibition of egfr n-glycosylation by tunicamycin enhances susceptibility of human non-small cell lung cancer cells to erlotinib,” *Cancer chemotherapy and pharmacology*, vol. 64, no. 3, pp. 539–548, 2009.
- [54] S. J. Marciniak, C. Y. Yun, S. Oyadomari, I. Novoa, Y. Zhang, R. Jungreis, K. Nagata, H. P. Harding, and D. Ron, “Chop induces death by promoting

- protein synthesis and oxidation in the stressed endoplasmic reticulum,” *Genes & development*, vol. 18, no. 24, pp. 3066–3077, 2004.
- [55] H. Liu, E. Miller, B. van de Water, and J. L. Stevens, “Endoplasmic reticulum stress proteins block oxidant-induced  $ca^{2+}$  increases and cell death,” *Journal of Biological Chemistry*, vol. 273, no. 21, pp. 12858–12862, 1998.
- [56] F. Chehrehasa, A. C. Meedeniya, P. Dwyer, G. Abrahamsen, and A. Mackay-Sim, “Edu, a new thymidine analogue for labelling proliferating cells in the nervous system,” *Journal of neuroscience methods*, vol. 177, no. 1, pp. 122–130, 2009.
- [57] R. Mussmann, M. Geese, F. Harder, S. Kegel, U. Andag, A. Lomow, U. Burk, D. Onichtchouk, C. Dohrmann, and M. Austen, “Inhibition of gsk3 promotes replication and survival of pancreatic beta cells,” *Journal of Biological Chemistry*, vol. 282, no. 16, pp. 12030–12037, 2007.
- [58] Z. Liu, K. Tanabe, E. Bernal-Mizrachi, and M. Permutt, “Mice with beta cell overexpression of glycogen synthase kinase-3 $\beta$  have reduced beta cell mass and proliferation,” *Diabetologia*, vol. 51, no. 4, pp. 623–631, 2008.
- [59] K. S. Polonsky, B. D. Given, L. J. Hirsch, H. Tillil, E. T. Shapiro, C. Beebe, B. H. Frank, J. A. Galloway, and E. Van Cauter, “Abnormal patterns of insulin secretion in non-insulin-dependent diabetes mellitus,” *New England Journal of Medicine*, vol. 318, no. 19, pp. 1231–1239, 1988.
- [60] L. E. Andersson, B. Valtat, A. Bagge, V. V. Sharoyko, D. G. Nicholls, P. Ravassard, R. Scharfmann, P. Spégel, and H. Mulder, “Characterization of stimulus-secretion coupling in the human pancreatic endoc- $\beta$ h1 beta cell line,” *PloS one*, vol. 10, no. 3, p. e0120879, 2015.
- [61] C. Weyer, T. Funahashi, S. Tanaka, K. Hotta, Y. Matsuzawa, R. E. Pratley, and P. A. Tataranni, “Hypoadiponectinemia in obesity and type 2 diabetes: close association with insulin resistance and hyperinsulinemia,” *The Journal of Clinical Endocrinology & Metabolism*, vol. 86, no. 5, pp. 1930–1935, 2001.
- [62] J. Y. Qin, L. Zhang, K. L. Clift, I. Hukur, A. P. Xiang, B.-Z. Ren, and B. T. Lahn, “Systematic comparison of constitutive promoters and the doxycycline-inducible promoter,” *PloS one*, vol. 5, no. 5, p. e10611, 2010.
- [63] M. Jain, A. Nijhawan, A. K. Tyagi, and J. P. Khurana, “Validation of housekeeping genes as internal control for studying gene expression in rice by quantitative real-time pcr,” *Biochemical and biophysical research communications*, vol. 345, no. 2, pp. 646–651, 2006.



# A

## Appendix

### A.1 Protocol for EndoC- $\beta$ H1 cell passaging

Cells were passaged once a week. Volumes needed depends on area of new container, see table A.3

1. Prepare new flasks/plates coated with fibronectin and ECM. See recipe table A.1
2. Incubate flasks/plates at 37°C at a minimum time of 1 hour.
3. Carefully remove culture media from flasks with cells and add Ca<sup>2+</sup>- and Mg<sup>2+</sup>-free PBS to wash cells.
4. Remove PBS and add 0.05% Trypsin/EDTA.
5. Incubate at 37°C for 3 min.
6. Add 20% FBS diluted in PBS to neutralize trypsin.
7. Move all liquid into a falcon tube and centrifuge (1200 rpm, 5 min).
8. Remove supernatant carefully. Add 1 mL culture media, see table A.2, and dissolve cell pellets by pipetting. Add culture media.
9. Count cells.
10. Remove coating media from prepared flasks/plates. Transfer cell suspension to flask to a final concentration of  $0.5 \times 10^6$  cells/mL.

**Table A.1:** Components and volumes needed in EndoC- $\beta$ H1 coating medium.

Coating medium (for immediate use):	For 50 mL
DMEM 4.5 g/L glucose (cold, 4°C)	50 mL
Penicillin/Streptomycin 1%	0.5 mL
Fibronectine 2 $\mu$ g/mL	0.1 mL
Extra Cellular Matrix (Matrigel) 1%	0.5 mL

**Table A.2:** Components and volumes needed in EndoC- $\beta$ H1 culture medium.

Culture medium	For 100 mL
DMEM low glucose (1 g/L)	100 mL
Penicillin/Streptomycin	1 mL
$\beta$ -mercaptoethanol	0.1 mL
Nicotinamide 10 mM	1 mL
Fatty acid free BSA fraction V	2 g
Transferrin 5.5 $\mu$ g/mL	10 $\mu$ L
Sodium selenite	10 $\mu$ L

**Table A.3:** Components and volumes needed in EndoC- $\beta$ H1 cell splitting depending on container area.

Component	T25	T75	T225
Coating media (mL)	2.5	5.0	15.0
PBS (Ca <sup>-</sup> /Mg <sup>-</sup> ) (mL)	5.0	10.0	30.0
0.05% Trypsin/EDTA (mL)	1.0	2.0	6.0
20% FBS (mL)	2.0	4.0	12.0
cell suspension (mL)	5.0	10.0	30.0

# B

## Appendix

### B.1 Protocol for MIN6 cell passaging

MIN6 cells were passaged when cells approached 70-80% confluency (after approximately 7 days). Culture media, see table B.1, was changed every second to third day. Volumes needed when passaging MIN6 cells depends on area of new container, see table B.2

1. Carefully remove culture media from flasks with cells and wash cells twice with  $\text{Ca}^{2+}$ - and  $\text{Mg}^{2+}$ -free PBS.
2. Remove PBS and add 0.125% trypsin-EDTA.
3. Incubate at 37°C for 3 min.
4. Tap well/flask firmly until cells come off.
5. Carefully rinse flask with culture media then transfer it to a falcon tube.
6. Spin down (140xg, 4 min).
7. Remove supernatant carefully. Add 1 mL culture media and dissolve cell pellets by pipetting. Add culture media.
8. Count cells.
9. Transfer cell suspension to flask/well to a final concentration of  $0.3 \times 10^6$  cells/mL.

**Table B.1:** Components and volumes needed in MIN6 culture medium.

Component	Volume (mL)
DMEM (4.5 g/L glucose, L-Glutamine)	500
FBS	50
Penicillin-Streptomycin	5
$\beta$ -mercaptoethanol (50 $\mu\text{M}$ )	0.5

**Table B.2:** Components and volumes needed in MIN6 cell splitting depending on container area.

Component	T25	T75	T225
PBS ( $\text{Ca}^-/\text{Mg}^-$ ) (mL)	5.0	10.0	30.0
0.125% Trypsin/EDTA (mL)	1.0	2.0	6.0
Cell suspension (mL)	5.0	10.0	30.0



# C

## Appendix

### C.1 Krebs-Ringer buffer

The following three solutions, see table C.1, can be prepared and kept during 6 months at +4°C. The solutions are to be mixed the same day according to table C.2.

**Table C.1:** Components and volumes in the three solutions needed for Krebs-Ringer buffer.

<b>Solution I</b>	<b>Solution II</b>	<b>Solution III</b>
5.38 g NaCl (460 mM) 200 mL H <sub>2</sub> O	1.61 g NaHCO <sub>3</sub> (96 mM) 300 mg KCl (20 mM) 76 mg MgCl <sub>2</sub> (4 mM) 200 mL H <sub>2</sub> O	117.6 mg CaCl <sub>2</sub> ·2H <sub>2</sub> O (4 mM) 200 mL H <sub>2</sub> O

**Table C.2:** Components and concentrations in Krebs-Ringer buffer.

Component	Concentration/percentage
BSA	0.2%
Eau maxima	25%
Solution I	25%
Solution II	25%
Solution II	25%
Hepes	10 mM



# D

## Appendix

### D.1 Adenoviral vector backbone

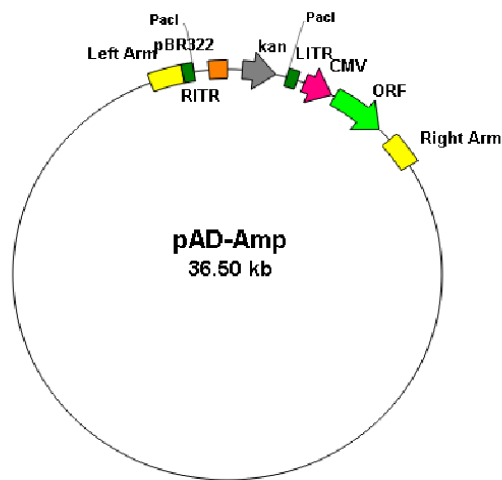


**Figure D.1:** Adenoviral vector backbone containing ORF under regulation of CMV promoter. Courtesy of [www.vigenebioscience.com](http://www.vigenebioscience.com), Copyright 2016 Vigene Biosciences Inc.